Zoological Journal of the Linnean Society, 2026, **208**(2), zlag163
https://doi.org/10.1093/zoolinnean/zlag163
Original Article

OXFORD

Echoes of Gondwana: Antarctic mite, *Maudheimia petronia* (Acari: Maudheimiidae), reveals deep-time isolation and highly modified mitochondrial transfer RNAs

Antonio Carapelli[1,2,*], Kyle Raymond Field[1,3], Francesco Nardi[1,2], Francesco Frati[1,2], Claudio Cucini[1,2], Rebecca Funari[1,2], Francesco De Giglio[4], Massimo Migliorini[1,2]

[1]Department of Life Sciences, University of Siena, Siena 53100, Italy
[2]National Biodiversity Future Center (NBFC), Palermo 90133, Italy
[3]Department of Environmental Sciences, Ca' Foscari University of Venice, Venezia Mestre 30170, Italy
[4]National Research Center for Agricultural Technologies (Agritech), Naples 80146, Italy

[*]Corresponding author. Department of Life Sciences, University of Siena, Via A. Moro 2, Siena 53100, Italy. E-mail: antonio.carapelli@unisi.it

Abstract

With an estimated 50000–100000 described species, mites represent the most diverse group of Chelicerata and include lineages adapted to some of the harshest environments on Earth, including those found in Antarctica. Here, we combine mitochondrial genomics, population genetics, and morphological analysis to investigate the Antarctic oribatid mite *Maudheimia petronia*, a putative Gondwanan relict species endemic to Victoria Land. Phylogenetic analyses based on mitochondrial protein-coding genes place *Maudheimia* within Brachypylina and support its affinity with Ceratozetoidea. Beyond species-level characterization, we also place our results in a broader phylogenetic context by discussing relationships within Sarcoptiformes and Oribatida to clarify higher-level evolutionary patterns. The mitochondrial genome exhibits a conserved protein-coding gene order but highly derived transfer RNAs, including extensive arm reduction, frequent mismatches, and overlapping genes. Population analysis of three isolated localities revealed geographically structured but conspecific populations, consistent with long-term persistence in Antarctic refugia. Morphological observations obtained through light and scanning electron microscopy confirmed the diagnostic characters of *M. petronia* and showed substantial morphological stability among populations. These results provide new insights into the evolutionary history, mitochondrial genome evolution, and historical biogeography of Antarctic oribatid mites.

Keywords Antarctica, Oribatida, biogeography, mitochondrial DNA, transfer RNA, taxonomy, phylogeny

Introduction

Mites exhibit extraordinary adaptations that enable them to colonize virtually every type of habitat, including some of the most extreme environments on Earth, most notably the polar regions (Block and Convey 1995, Søvik 2004, Teets and Denlinger 2014). Their resilience allows them to withstand harsh environmental pressures, including extreme temperatures, repeated freeze–thaw cycles, prolonged desiccation, and the constraints of a short and often unpredictable growing season. However, recent work has challenged the traditional view of Antarctic terrestrial arthropods as being exposed exclusively to uniformly extreme air temperatures, showing that microhabitats, such as soils and ponds, can experience markedly warmer and more thermally stable conditions than the surrounding atmosphere (Cucini *et al.* 2022).

Increasing evidence accumulated over the last two decades has substantially reshaped our understanding of the history of Antarctic terrestrial biota, supporting the persistence of diverse endemic lineages through multiple glacial cycles in long-term ice-free refugia, rather than repeated recent recolonization events (Convey and Stevens 2007, Convey *et al.* 2008, 2020). Within this framework, the persistence of Antarctic

Received: 20 January 2026. **Revised:** 3 September 2026. **Accepted:** 7 September 2026
© The Author(s) 2026. Published by Oxford University Press on behalf of The Linnean Society of London.
This is an Open Access article distributed under the terms of the Creative Commons Attribution License (https://creativecommons.org/licenses/by/4.0/), which permits unrestricted reuse, distribution, and reproduction in any medium, provided the original work is properly cited.

Downloaded from academic.oup.com/zoolinnean/article/208/2/zlag163/9003135 by Università degli studi di Siena user on 28 October 2026

soil arthropods has been linked to ecological specialization and local adaptation, including traits that enhance survival in severe environmental conditions.

Endemic to Antarctica, the Sarcoptiform genus *Maudheimia* Dalenius & Wilson, 1958 (Oribatida: Maudheimiidae) is an oribatid taxon associated with high-elevation epilithic rocky habitats, characterized by a weakly sclerotized exoskeleton and a lichen-based diet (Marshall and Coetzee 2000). Currently, the genus is the sole representative of the family Maudheimiidae and comprises four recognized allopatric species distributed across isolated regions of continental Antarctica, spanning three subdivisions of the Antarctic Conservation Biogeographic Regions (ACBRs; Terauds and Lee 2016). *Maudheimia marshalli* Coetzee, 1997, *Maudheimia wilsoni* Dalenius & Wilson, 1958, and *Maudheimia tanngardensis* Coetzee, 1997 all occur within Dronning Maud Land (ACBR 6), where their distributions are separated by three major glaciers. *Maudheimia petronia* Wallwork, 1962 is endemic to Victoria Land and occurs in both North and South Victoria Land (ACBRs 8 and 9, respectively; Marshall and Coetzee 2000; Fig. 1). The marked geographical isolation of these species has long been considered an important factor shaping the evolutionary history of the genus (Coetzee and Weigmann 2012).

Modern lineages are believed to descend from ancestors that inhabited Antarctica before the break-up of Gondwana during the Early Cretaceous (~145–100 Mya; Pugh and Convey 2008). Following the isolation of Antarctica and the progressive cooling of the continent, these mites are thought to have persisted through successive glacial periods within isolated ice-free refugia (Marshall and Coetzee 2000, Ross *et al.* 2025). Subsequent population fragmentation is likely to have promoted genetic bottlenecks and episodes of speciation associated with glacial maxima and shifting ice-sheet dynamics during interglacial periods (Marshall and Coetzee 2000).

Following adaptation to Antarctic environmental conditions, *Maudheimia* species exhibit a suite of ecological and physiological traits that might enhance survival under extreme environmental stress. They occur in multi-instar aggregations characterized by synchronized development from egg through protonymph, deutonymph, and tritonymph, with at least one moult occurring each austral summer. This developmental pattern implies a minimum life cycle of ~5 years (from egg to egg), and all life stages appear capable of overwintering. Synchronous moulting has been proposed as a mechanism reducing juvenile mortality in severe environmental conditions (Marshall and Convey 1999). Experimental studies have shown that *M. wilsoni* can supercool to approximately −30°C (Sømme *et al.* 1993), approaching the supercooling capacity of pure-water droplets of comparable volume (Bigg 1953, Block and Young 1979). In small Antarctic mites, such pronounced supercooling capacity is facilitated by the synthesis and accumulation of cryoprotective compounds, including glycerol, as documented in *Alaskozetes antarcticus* (Michael, 1903) (Young and Block 1980). A similar cryoprotective mechanism might therefore also be present in species of *Maudheimia*, although this remains to be demonstrated experimentally. From a systematic perspective, the genus was established by Dalenius and Wilson (1958) for *M. wilsoni* and was initially considered closely related to *Scheloribates* within the family Scheloribatidae. A few years later, Wallwork (1962) described *M. petronia* from Victoria Land. Owing to differences in the structure of the octotaxic organs (porose areas in *Maudheimia vs*. sacculi in *Scheloribates*), Balogh and Balogh (1984, 1992) proposed the erection of the family Maudheimiidae. Subsequently, Coetzee (1997) revised the genus, describing *M. marshalli* and *M. tanngardensis*, and transferred *Maudheimia* to Ceratozetoidea, a placement later reaffirmed by Coetzee and Weigmann (2012).

Morphology-based phylogenetic analyses recovered all recognized *Maudheimia* species within a strongly supported clade and suggested a stepwise pattern of divergence in which *M. petronia* occupies a basal position, whereas *M. marshalli* and *M. wilsoni* are more closely related to each other than either is to *M. tanngardensis*. The congruence between phylogenetic topology and species distributions suggests diversification during the Plio-Pleistocene, driven by repeated glacial cycles and long-term isolation in refugia. Collectively, phylogenetic, biogeographical, and ecological evidence supports the interpretation of *Maudheimia* as a relict Antarctic lineage (Coetzee and Weigmann 2012).

More broadly, phylogenetic studies of Sarcoptiformes and Oribatida have revealed deep lineage diversification and substantial heterogeneity in evolutionary rates, providing a comparative framework for assessing the evolutionary placement of Antarctic taxa such as *Maudheimia*. Much of this recent progress has been driven by the increasing use of molecular data. In recent decades, the evolutionary trajectories of Antarctic terrestrial invertebrates have been explored increasingly using molecular tools, particularly in Collembola (Stevens *et al.* 2006, McGaughran *et al.* 2010, Collins *et al.* 2019, 2020, Carapelli *et al.* 2020, Boschi *et al.* 2025) and mites (Stevens and Hogg 2006, Mortimer *et al.* 2011, Brunetti *et al.* 2021, Collins *et al.* 2023). Most studies rely on mitochondrial DNA (mtDNA), whose lineage-specific molecular features and gene order are widely used in population genetics, species delimitation, and phylogenetics. With few exceptions, animal mitochondrial genomes are circular molecules of ~16 kb in size, encoding 37 genes: 13 protein-coding genes (PCGs), two ribosomal RNA-coding genes and 22 transfer RNA (tRNA)-coding genes, plus a major non-coding regulatory region involved in mtDNA replication and transcription (Clayton 1992, Zhang and Hewitt 1997, Boore 1999, Podsiadlowski *et al.* 2006). Despite this conserved gene complement, mites exhibit remarkable mitochondrial genome diversity, including extensive gene rearrangements and highly modified tRNAs (Domes *et al.* 2008, Klimov and O'Connor 2009, Yuan *et al.* 2010, Xue *et al.* 2016, Arribas *et al.* 2020, Warren and Sloan 2021, Aydemir 2024).

In contrast to the ecological and biogeographical significance of the genus, important aspects of its evolutionary history and systematic relationships remain poorly understood. To improve our understanding of these aspects, we adopted a multidisciplinary approach combining morphology and mtDNA analyses of three populations of *M. petronia* from Victoria Land. This study provides the first mitochondrial

Downloaded from academic.oup.com/zoolinnean/article/208/2/zlag163/9003135 by Università degli studi di Siena user on 28 October 2026

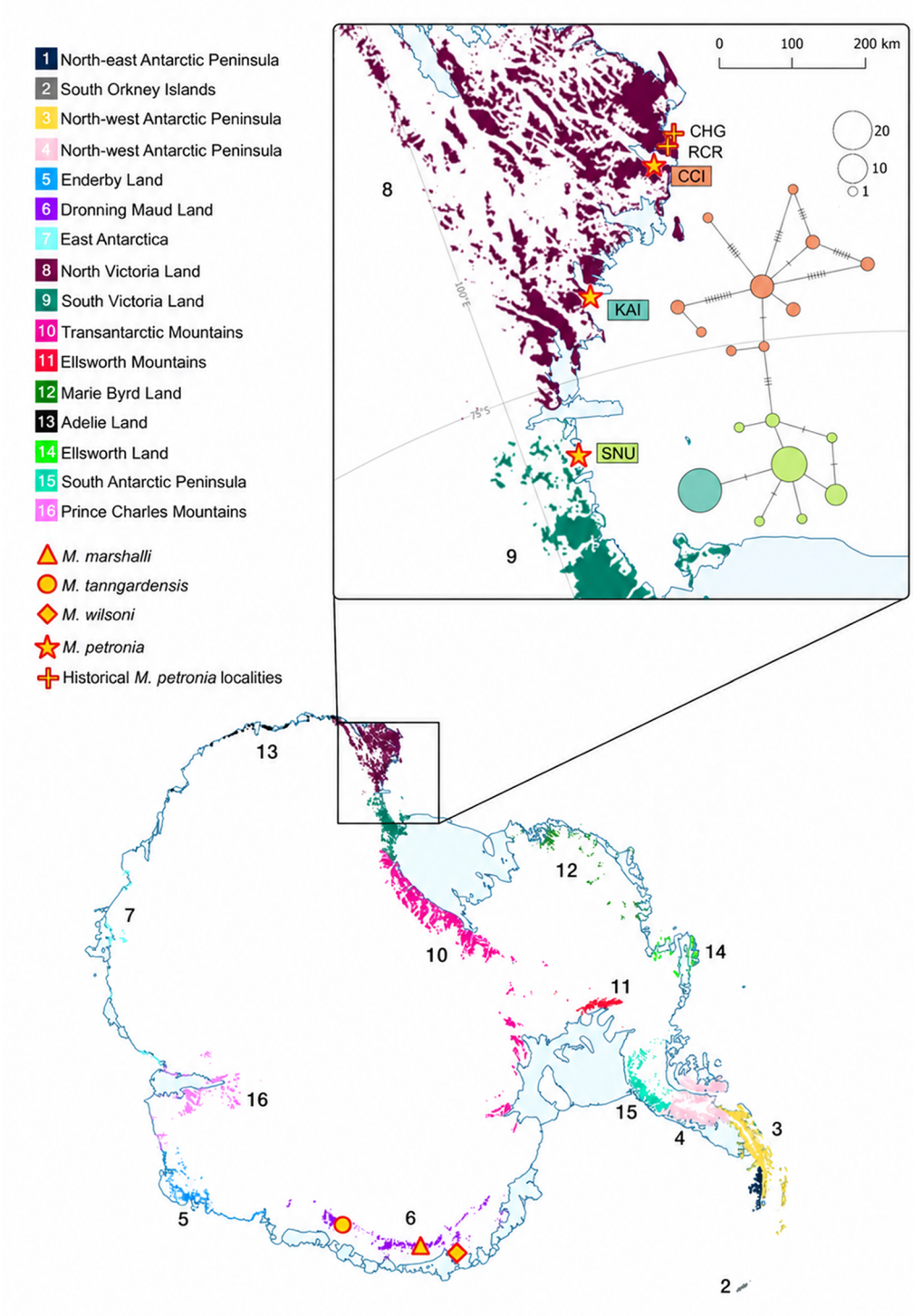


Figure 1 Map of Antarctica and 16 Antarctic Conservation Biogeographical Regions (ACBRs) Terauds and Lee (2016) using the Quantarctica 3 QGIS package (Matsuoka *et al.* 2018). Locations of all four species of *Maudheimia* are labelled, including the three *M. petronia* sampling localities included in this study, in addition to historical sampling sites (CHG, Cape Hallett; RCR, Redcastle Ridge) to represent the entire sampled distribution of this species. Sixty-six *cox1* barcode sequences from the three sampling sites were used to create a minimum spanning haplotype network, showing haplotype diversity within and between populations. Population abbreviations are as follows: CCI, Crater Cirque; KAI, Kay Island; SNU, Starr Nunatak.

genome sequence and population-level DNA barcode dataset for the species. Specifically, our aims were as follows: (i) to assess genetic variability among populations; (ii) to characterize mitochondrial genome features; (iii) to clarify the phylogenetic placement of *Maudheimia* within Oribatida; and (iv) to re-examine key morphological traits using light

Downloaded from academic.oup.com/zoolinnean/article/208/2/zlag163/9003135 by Università degli studi di Siena user on 28 October 2026

and electron microscopy, evaluating their congruence with previous species descriptions (Dalenius and Wilson 1958, Wallwork 1962, Coetzee 1997).

Materials and methods

Sample collections

Samples of *M. petronia* were collected during the 2017–2018 and 2018–2019 Antarctic summers in three localities of Victoria Land (Table 1; Fig. 1). Specimens were initially identified and subsequently stored at −80°C until molecular analysis, while a subset of specimens was preserved in 70% ethanol for morphological examination.

Mitochondrial genome sequencing, assembly, and annotation

Seven individuals sampled in Starr Nunatak were pooled to obtain a sufficient DNA concentration required for the high-throughput sequencing workflow. Their DNA was extracted using the QIAmp® UCP DNA kit. Total DNA was normalized and sequenced at Macrogen Europe using TruSeq Nano DNA chemistry on an Illumina HiSeq 2500 platform, together with additional samples not reported in this study (for further details, see Carapelli *et al.* 2020, 2021, Cucini *et al.* 2021a, 2021b). Resulting reads were quality checked using FastQC (v.0.11.9; https://www.bioinformatics.babraham.ac.uk/projects/fastqc/) and subsequently assembled with NOVOPlasty v.3.8.3 (Dierckxsens *et al.* 2017). Genome assembly was performed using a single *cytochrome c oxidase subunit I* (*cox1*) sequence (amplified as described in the 'Population genetic analyses' section) as seed. Initial assemblies were generated under default parameters and subsequently used as a reference to generate a subset of reads enriched for mitochondrial sequences using the *filter_reads.pl* script provided with the NOVOPlasty package. Final assemblies were then produced using this enriched read set. The resulting contigs were compared with assemblies generated using MEGAHIT (Li *et al.* 2015) and curated manually to obtain complete mitochondrial genome sequences. Single-nucleotide ambiguities were resolved using a majority-rule approach by remapping reads to ambiguous regions with BBMap v.38.84 (sourceforge.net/projects/bbmap/) and visualizing alignments in IGV v.2.8.2 (Robinson *et al.* 2011). The complete mitochondrial genome sequence was deposited in GenBank under accession number PX633171, and the corresponding raw sequencing reads were deposited in the Sequence Read Archive (SRA) at NCBI under accession number SRP289641.

The mitochondrial genome of *M. petronia* (Fig. 2) was initially annotated automatically using MITOS2 through the Galaxy Server (Al Arab *et al.* 2017, Donath *et al.* 2019). To refine this preliminary annotation, tRNA genes were predicted using tRNAscan-SE (Lowe and Eddy 1997) and ARWEN (Laslett and Canbäck 2008), resulting in identification of 18 of the 22 expected mitochondrial tRNAs. The four genes not detected automatically (*trnA*, *trnH*, *trnV*, and

Table 1 Information on collection sites, sample size, and population genetics parameters.

Collection site		Coordinates	N	N_H	N_p	H	h	π	$\theta(p)$	$\theta(S)$
Kay Island	KAI	74°04′14″ S, 165°18′60″ E	22	1	0	A(22)	.000 ± .000	.000 ± .000		
Starr Nunatak	SNU	75°53′57″ S, 162°35′08″ E	25	7	7	B(14), C(5), D(2), E(1), F(1), G(1), H(1)	.660 ± .092	.0016 ± .0012	1.0600 ± 0.7260	1.8538 ± 0.8882
Crater Cirque	CCI	72°37′52″ S, 169°22′22″ E	19	10	6	I(6), J(2), K(2), L(2), M(2), N(1), O(1), P(1), Q(1), R(1)	.889 ± .0562	.0096 ± .0053	6.3743 ± 3.1602	10.3001 ± 3.8512

Abbreviations: H, haplotype labels; h, haplotype diversity; N, number of individuals; N_H, number of haplotypes; N_p, number of nucleotide polymorphisms; π, nucleotide diversity; $\theta(p)$, mean number of pairwise differences per population; $\theta(S)$, mean number of segregating sites per population.

Downloaded from academic.oup.com/zoolinnean/article/208/2/zlag163/9003135 by Università degli studi di Siena user on 28 October 2026

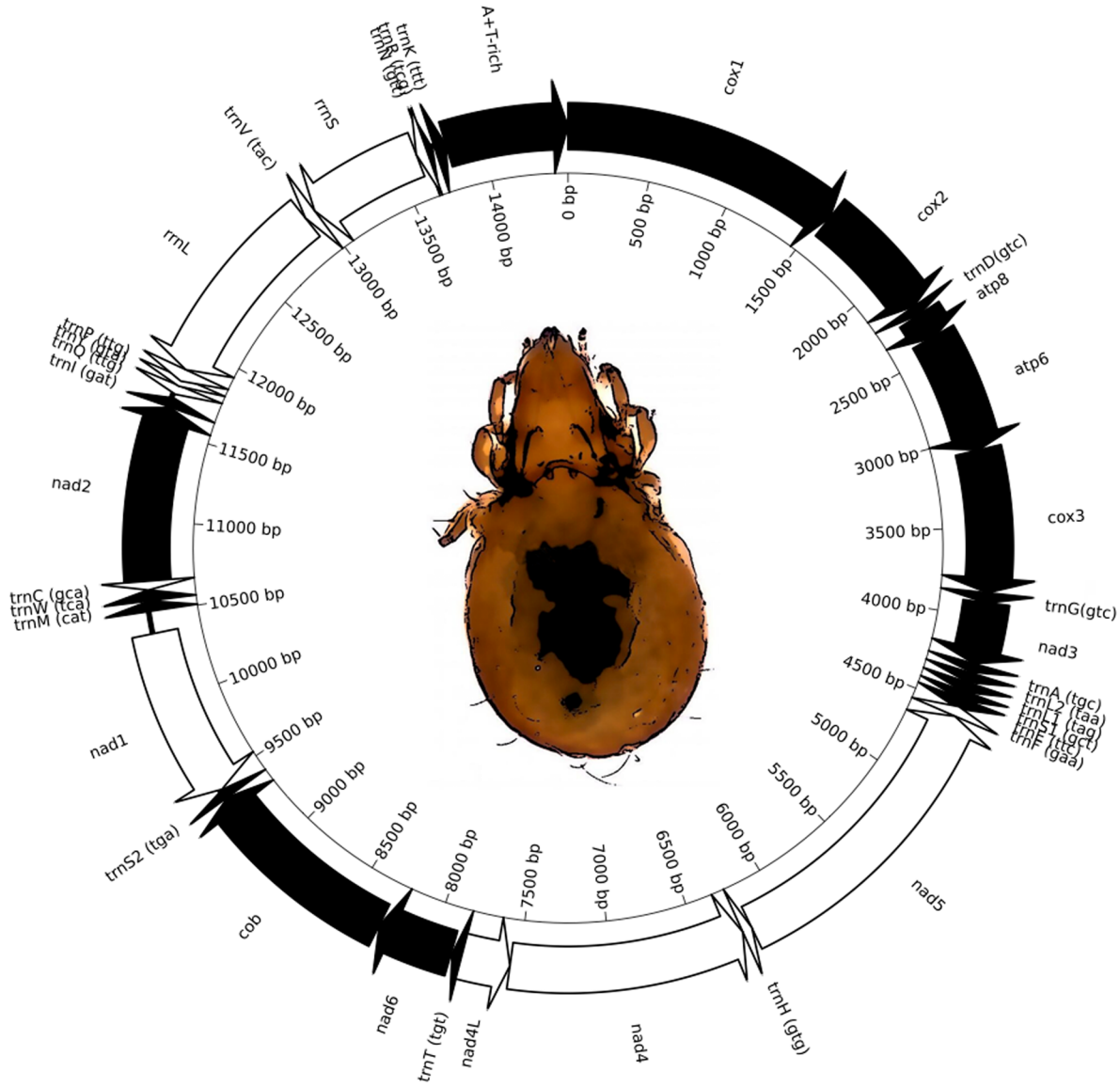


Figure 2 Map of the circular mitochondrial genome of *M. petronia* with the typical set of 37 genes highlighted, including two ribosomal RNAs (*rrnS* and *rrnL*), 13 protein-coding genes for subunits of the respiratory enzyme complexes (*atp6*, *atp8*, *cox1–3*, *cob*, *nad1–6*, and *nad4L*), and 22 transfer RNAs (*trnX*).

trnY) were subsequently located through manual inspection. The putative secondary structures of these tRNAs, together with those of the 18 tRNAs identified by MITOS2, were reconstructed using the software VARNA 9–93 (Darty *et al.* 2009; Fig. 3).

For comparative analysis of the mitochondrial gene order, mitogenomes of six Brachypylina mitogenomes were retrieved from GenBank and automatically annotated using MITOS2 within the Galaxy Server (Al Arab *et al.* 2017, Donath *et al.* 2019) to ensure methodological consistency. The mitogenomes of *Oppia nitens* and *Paraleius leontonychus* were excluded from downstream analyses because MITOS2 and/or previous studies (Schäffer *et al.* 2018) failed to identify the complete set of mitochondrial tRNA genes. Gene order rearrangements and synteny were inferred using CREx (Bernt *et al.* 2007).

Phylogenetic analyses

All PCGs from 51 Sarcoptiformes complete mitochondrial genomes, along with three outgroup sequences from Trombidiformes available in GenBank as of September 2025, were downloaded. Nine of the 13 sequences (accession numbers: MF083732–MF083739 and CM003133) for *Sarcoptes scabiei* were excluded from the analyses owing to taxonomic overrepresentation, leading to a final dataset of 45 sequences (Supplementary Table S1). Protein-encoding gene sequences were separated into 13 FASTA files using the function EZsplit from the Ezmito2 Web Server (Cucini *et al.* 2026). In addition, four unverified sequences corresponding to *Ardeacarus ardeae*, *Carpoglyphus lactis*, *O. nitens*, and *Platynothrus peltifer* were annotated, at least for their PCGs, using the MITOS2 tool through the Galaxy Server (Donath *et al.* 2019) and added to the remaining dataset. FASTA files were then aligned using

Downloaded from academic.oup.com/zoolinnean/article/208/2/zlag163/9003135 by Università degli studi di Siena user on 28 October 2026

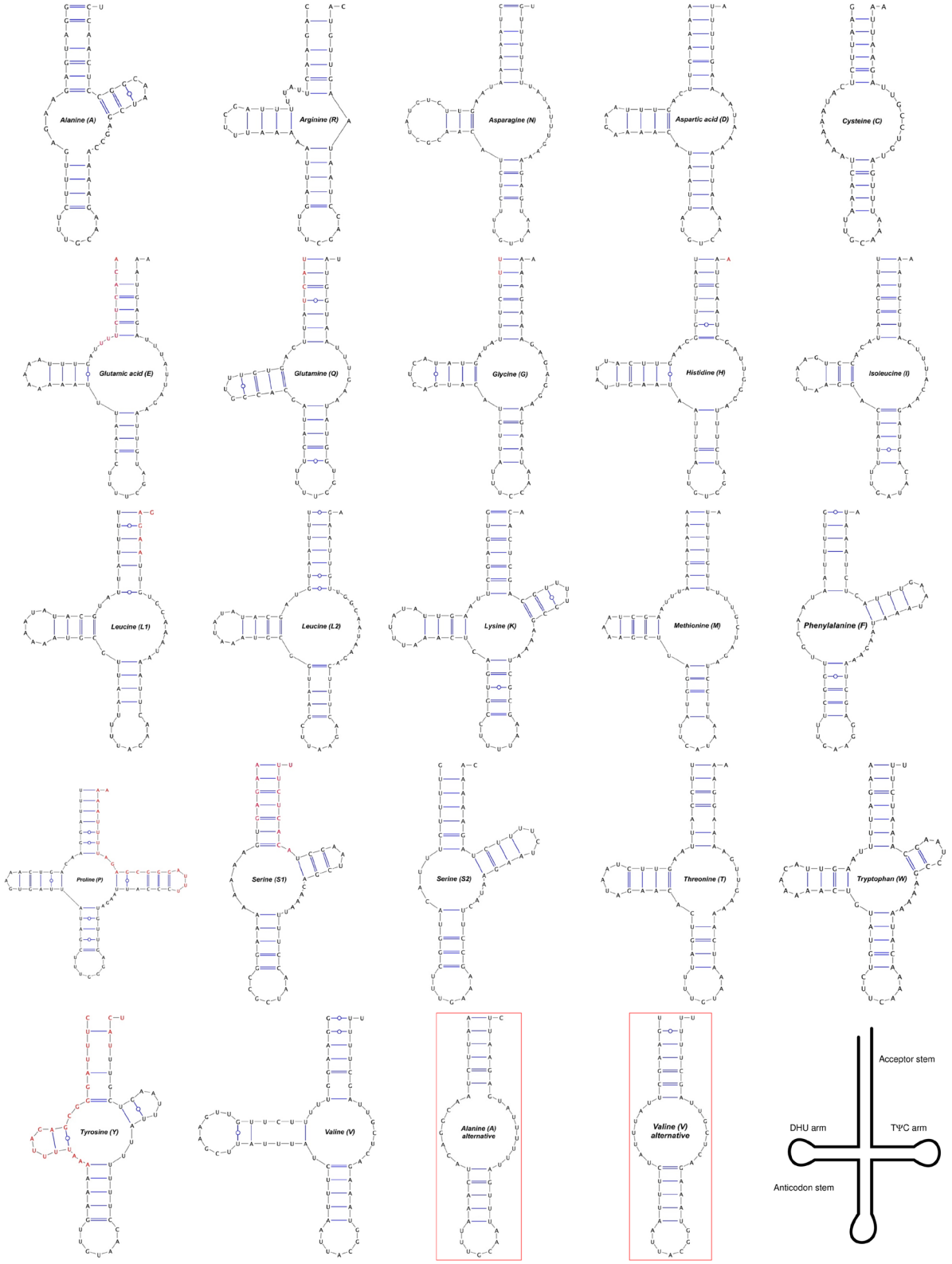


Figure 3 Predicted secondary structures of the mitochondrial tRNAs of *M. petronia*. Nucleotides shared between tRNA-encoding genes and neighboring genes oriented on the same strand are highlighted in red (see also Table 2). Alternative genes with highly miniaturized secondary structures for tRNA A and tRNA V are shown in boxes.

CLUSTAL OMEGA (Sievers and Higgins 2018) into 13 matrices, each corresponding to one mtDNA gene to check for possible errors of gene orientation. Then, the 13 files were processed through the EZpipe tool of EZMITO2 (Cucini *et al.* 2026) to realign the sequences, remove unalignable/hypervariable stretches, and finally, to obtain the concatenated alignment for the whole dataset (three matrices: codons, 1&2_only, and aa). The number of included positions per gene in the

Downloaded from academic.oup.com/zoolinnean/article/208/2/zlag163/9003135 by Università degli studi di Siena user on 28 October 2026

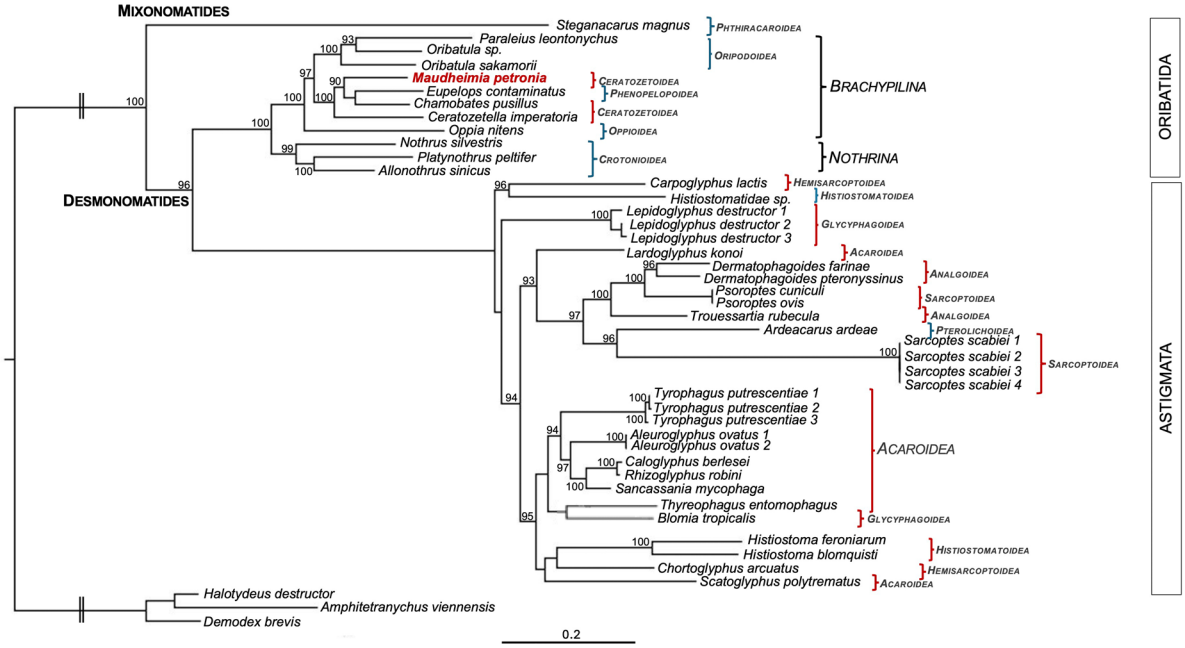


Figure 4 Mito-phylogenetic relationships among Sarcoptiformes mite taxa inferred from IQ-TREE analyses of first and second nucleotide positions of 13 protein-coding genes. Only bootstrap values >89 are shown at the nodes.

alignment is reported in Supplementary Table S2. The final dataset consisted of 42 ingroup and 3 outgroup taxa and was subjected to phylogenetic analysis in IQ-TREE v.3 (Wong *et al.* 2026), using the best-fitting evolutionary model for each partition and estimating separate evolutionary rates among partitions. These latter were defined by gene for the amino acid dataset, by gene and codon positions (first and second) for the 1&2-only nucleotide dataset, and by gene and all three codon positions for the complete nucleotide dataset. The best evolutionary models were chosen with MODEL FINDER PLUS. Nodal supports were established by running 1000 ultrafast bootstraps and SH-aLRT iterations. The three phylogenetic trees were edited graphically with FIGTREE (Rambaut 2018) and are reported in Fig. 4 and Supplementary Figs S1 and S2, respectively.

Population genetic analyses

A total of 66 individuals from three populations (Fig. 1; Table 1) were sequenced for the barcoding fragment of the mitochondrial *cox1* gene. Total DNA from each specimen was extracted using the Wizard SV Genomic DNA Purification System (Promega, Madison, WI, USA) and eluted in 50 µL ddH_2O. PCR amplification was then performed in a T100 (Bio-Rad, Hercules, CA, USA) thermal cycler. The mtDNA barcode region, part of *cox1* (Hebert *et al.* 2003), was amplified using the primers 5′-GGTCAACAAATCATAAAGATATTGG-3′ (LCO, forward) and 5′-TAAACTTCAGGGTGACCAAAAAATCA-3′ (HCO, reverse) (Folmer *et al.* 1994). Reactions were run using 2.5 µL of extracted DNA, 0.5 µM of each primer, 0.2 mM of each dNTP, 2.5 mM $MgCl_2$, 5 µL of Green GoTaq Flexi buffer, and 0.125 µL of GoTaq Flexi DNA Polymerase (Promega), in a total volume of 25 µL. Amplification of the *cox1* fragment was obtained using the following cycling conditions: (i) 95°C for 5 min; (ii) 35 cycles of 95°C for 1 min, 50°C for 1 min, 72°C for 1 min 30 s; and (iii) 72°C for 7 min. PCR products were purified using the Wizard SV Gel and PCR Clean-up kit (Promega), then quantified using Nanodrop One (Thermo Fisher Scientific, Waltham, MA, USA). Upon successful Sanger sequencing of both forward and reverse strands obtained at the BMR Genomics facility (Padua, Italy), the resulting electropherograms were quality controlled using SEQUENCHER v.4.4.2 (Gene Codes Corporation, Ann Arbor, MI, USA) and assembled into consensus sequences. Sequences were aligned using ALIVIEW v.1.28 (Larsson 2014) and trimmed manually, resulting in a 657 bp, indel-free matrix. Haplotype frequencies were determined using the online tool DNAcollapser (available at: https://users-birc.au.dk/~palle/php/fabox/index.php). Individual haplotype sequences were then assigned a label (Table 1) and submitted to GenBank, where they are available under accession numbers PX498765–PX498782. A minimum spanning haplotype network (Fig. 1) was constructed using POPART (Leigh and Bryant 2015) to infer phylogenetic relationships between populations. For additional population genetics analyses, ARLEQUIN v.3.11 (Excoffier *et al.* 2005) was used to determine haplotype (h) and nucleotide (π) diversity indices, in addition to the mean number of pairwise differences (θ) and segregating sites (θS) (Table 1).

Morphological analysis

Ten individuals from each sampling site were used for taxonomic identification and morphological analysis. Morphological comparisons, measurements, and optical images were carried out with a Nikon Eclipse Ci-L plus (Kanagawa, Japan) and a Zeiss Axio Zoom V16 (Oberkochen, Germany) microscope. The resulting images were processed with ZERENE STACKER for photo stacking. Subsequently, to observe morphological traits not visible with optical microscopy, some *M. petronia* specimens were dehydrated through a graded ethanol series and dried

Downloaded from academic.oup.com/zoolinnean/article/208/2/zlag163/9003135 by Università degli studi di Siena user on 28 October 2026

using a critical point dryer (Balzers CDP 01), prior to gold coating using a Balzers Med 010 (FEI Company, Hillsboro, OR, USA). Prepared specimens were examined using a FEI Quanta 400 (FEI Company) scanning electron microscope operating at 20 kV.

Results

Mitochondrial genome features

The *M. petronia* mtDNA is a circular molecule of 14468 nucleotides that contains the typical set of 37 genes usually found in Metazoa (Fig. 2). Base composition is biased towards adenines and thymines (AT% = 68), with positive AT- and CG-skews on the J-strand (0.16 and 0.12, respectively). Nine of the 13 PCGs start with a standard methionine codon (ATA or ATG), whereas *cox2*, *cox3*, *nad2*, and *nad5* initiate with ATT, which encodes isoleucine. Stop codons are either complete (TAA or TAG, as in *atp8*, *cox1*, *nad1*, *nad2*, *nad4*, and *nad5*) or incomplete (TA- or T--, as in *atp6*, *cob*, *cox2*, *cox3*, *nad3*, *nad4L*, and *nad6*). Small overlaps occur between adjacent genes located on the opposite or, in a few cases, the same strand (Table 2). Intergenic regions vary in length from a few nucleotides to 123 nucleotides at the *nad1–trnM* junction (Table 2).

Table 2 Annotation, gene orientation, start and stop codons of PCGs and other features of the mitochondrial genome of *M. petronia*.

Gene	Start	End	Strand	Start codon	Stop codon	Anticodon	Intergenic spacer/overlap
cox1	1	1542	+	ATA	TAA		
cox2	1543	2212	+	ATT	T--		0
trnD(gtc)	2213	2265	+			2242–2244	0
atp8	2266	2415	+	ATA	TAA		0
atp6	2409	3076	+	ATG	TA-		−7
cox3	3077	3861	+	ATT	TA-		0
trnG(tcc)	3862	3917	+			3893–3895	0
nad3	3916	4255	+	ATG	T--		−2
trnA(tgc)	4256	4304	+			4274–4276	0
trnL2(taa)	4309	4363	+			4329–4331	4
trnL1(tag)	4364	4420	+			4395–4397	0
trnS1(gct)	4416	4467	+			4435–4437	−5
trnE(ttc)	4459	4517	+			4491–4493	−9
trnF(gaa)	4505	4560	−			4538–4540	−13
nad5	4562	6196	−	ATT	TAA		1
trnH(gtg)	6196	6250	−			6219–6221	−1
nad4	6251	7552	−	ATG	TAG		0
nad4L	7553	7821	−	ATA	TA-		0
trnT(tgt)	7821	7875	+			7851–7853	−1
nad6	7881	8302	+	ATG	TA-		5
cob	8303	9396	+	ATG	TA-		0
trnS2(tga)	9397	9447	+			9415–9417	0
nad1	9450	10382	−	ATA	TAA		2
trnM(cat)	10506	10562	+			10536–10538	123
trnW(tca)	10563	10622	+			10593–10595	0
trnC(gca)	10622	10670	−			10645–10647	−1
nad2	10661	11632	+	ATT	TAG		−10
trnI(gat)	11635	11688	+			11664–11666	2
trnQ(ttg)	11711	11762	−			11732–11734	22
trnY(gta)	11759	11809	−			11783–11785	−4
trnP(tgg)	11789	11856	−			11826–11828	−21
rrnL	11857	12920	−				0
trnV(tac)	12921	12984	−			12944–12946	0
rrnS	12985	13620	−				0
trnN(gtt)	13621	13681	−			13646–13648	0
trnR(tcg)	13666	13715	+			13697–13699	−16
trnK(ttt)	13728	13790	+			13760–13762	12
A + T-rich	13791	14468					0

Downloaded from academic.oup.com/zoolinnean/article/208/2/zlag163/9003135 by Università degli studi di Siena user on 28 October 2026

Comparative analyses of mitochondrial gene rearrangements in Brachypylina

Comparative analysis of mitochondrial gene order is inferred among Brachypylina species (Supplementary Table S1) and reveals a generally conserved genomic organization with limited structural variation, especially for PCGs. There are two larger gene blocks that are invariable within the dataset: *cox1–cox2–trnD–atp8–atp6–cox3* and *trnP–rrnL–trnV–rrnS–trnN–trnR*. The gene order observed in *M. petronia* is nearly identical to the Acari mitotype M42 [one of 67 configurations recognized by Aydemir (2024)] previously reported for *Oribatula* sp., differing by only a single rearrangement, in which *trnE* is positioned within the segment *trnS1–trnE–trnF* instead of *trnR–trnE–trnK*. The mitochondrial genome of *M. petronia* shows an identical gene arrangement to that of the oribatid mite *Chamobates pusillus* (GenBank accession: LC817328), which was not included in the comparison by Aydemir (2024). Pairwise comparisons of gene order using CREx identified pairwise rearrangement distances ranging from zero to five among the analysed taxa (Supplementary Table S3). *Maudheimia petronia* and *C. pusillus* showed the lowest distance values, whereas *Oribatula sakamorii* displayed the highest distances relative to the remaining taxa (Supplementary Table S3).

Protein-encoding and transfer RNA genes mapping and structure

Several of the predicted tRNAs deviate from the canonical cloverleaf structure expected for metazoan mitochondrial tRNAs (Fig. 3): tRNA C lacks both the T and D arms, whereas many others (except tRNA K, tRNA P, and tRNA W) retain only one of these arms, and some of these latter (i.e. tRNA A and tRNA V) have alternatives in other regions of the genome (see Fig. 3). As for stems, 8.7% of the total (357) expected pairings of nucleotides within helices are mismatches. Gene overlaps are frequent, spanning from 2 to 21 nucleotides and, unexpectedly, also involving neighbouring tRNA-encoding genes or PCGs and tRNA-encoding genes oriented on the same strand (Table 2). The arbitrary attribution of 'shared' stretches of sequences to one of the two neighbour genes results in the disruption of the acceptor arm helix (tRNA L1, tRNA P, tRNA S1, and tRNA Y; Fig. 3) or of the standard start/stop codon translational signal of *atp6*, *atp8*, *nad4*, *nad3*, and *nad5*.

Phylogeny of Sarcoptiformes

Phylogenetic analyses of Sarcoptiformes based on mitochondrial PCGs yield largely congruent topologies, particularly at the deepest nodes. All analyses consistently recover a well-supported dichotomy separating Astigmata and Oribatida. The sole exception is the oribatid *Steganacarus magnus* (Mixonomatida), which occupies a basal position relative to the remaining ingroup taxa, forming the base of the Desmonomatida clade and falling outside the otherwise monophyletic Oribatida (Fig. 4). These relationships indicate that astigmatid mites originated within oribatid mites, rendering Oribatida paraphyletic. Our results support the monophyly of Brachypylina and Nothrina and indicate that Astigmata emerge within a paraphyletic Oribatida *s.l.* Within Brachypylina, the relationships among the analysed species do not support the monophyly of Ceratozetoidea, because *Eupelops contaminatus* (Phenopelopoidea) is nested within Ceratozetoidea, rendering this superfamily paraphyletic. A sister-group relationship between *M. petronia* and the clade (*C. pusillus* + *E. contaminatus*), with *Ceratozetella imperatoria* as the most basal taxon, is slightly preferred, being recovered in the amino acid and first and second codon-positions-only trees, but not in the all-codon-position tree (Fig. 4; Supplementary Figs S1, S2). In our phylogenetic inference, one difference among the trees concerns the relative positions of *C. lactis* + Histiostomatidae sp. and the cluster representing the three *Lepidoglyphus destructor* specimens. In all topologies, these *L. destructor* sequences are consistently placed as basal lineages within Astigmata, but their positions relative to *C. lactis* + Histiostomatidae sp. are reciprocally exchanged depending on whether the tree is based on all codon positions, first and second codon positions only, or the translated amino acid sequences.

Within Astigmata, Psoroptidia and Acaroidea are recovered as well-supported monophyletic groups, whereas Acaridia and Glycyphagoidea appear paraphyletic. Indeed, within Glycyphagoidea, the three *L. destructor* sequences occur on branches distant from *Blomia tropicalis* and *Chortoglyphus arcuatus*. Within Acaroidea, the subfamily Rhizoglyphinae is monophyletic, whereas Tyrophaginae is not. Interestingly, Histiostomatidae sp. (Histiostomatoidea) clusters with *C. lactis* (Hemisarcopteroidea) rather than with the other two *Histiostoma* species (*Histiostoma blomquisti* and *H. feroniarum*).

Population genetics

Our analyses compare 66 *cox1* barcode fragments representing specimens from three distinct, isolated populations in Victoria Land (Fig. 1; Table 1). In total, 18 haplotypes are present, of which none is shared between localities. A single haplotype is recovered from 22 specimens from Kay Island, resulting in zero diversity indices. Crater Cirque has a total of 10 haplotypes present, sourced from 19 specimens, and shows the highest values in both haplotype diversity (0.889) and nucleotide diversity (0.0096). Seven haplotypes are obtained from Starr Nunatak specimens, with haplotype diversity of 0.66 and nucleotide diversity of 0.0016 (Table 1).

Intrapopulation *p*-distances (the proportion of nucleotide sites that differ between two aligned sequences) of Starr Nunatak haplotypes range from 0.15% to 0.76% (Supplementary Table S4). In contrast, the intrapopulation *p*-distances of Crater Cirque haplotypes range from 0.15% to 2.44%, exceeding the maximum interpopulation *p*-distance of 2.13%. Between populations, both the number of haplotypes and the extent of molecular variability differ markedly, indicating substantial differences in population structure or potential biases attributable to non-random sampling. The haplotype network reveals a clear geographical structuring of mitochondrial lineages, which are divided into two main groups: the first comprises specimens from Starr Nunatak and Kay Island, whereas the second subnetwork includes all haplotypes from the northern population of Crater Cirque (Fig. 1).

Downloaded from academic.oup.com/zoolinnean/article/208/2/zlag163/9003135 by Università degli studi di Siena user on 28 October 2026

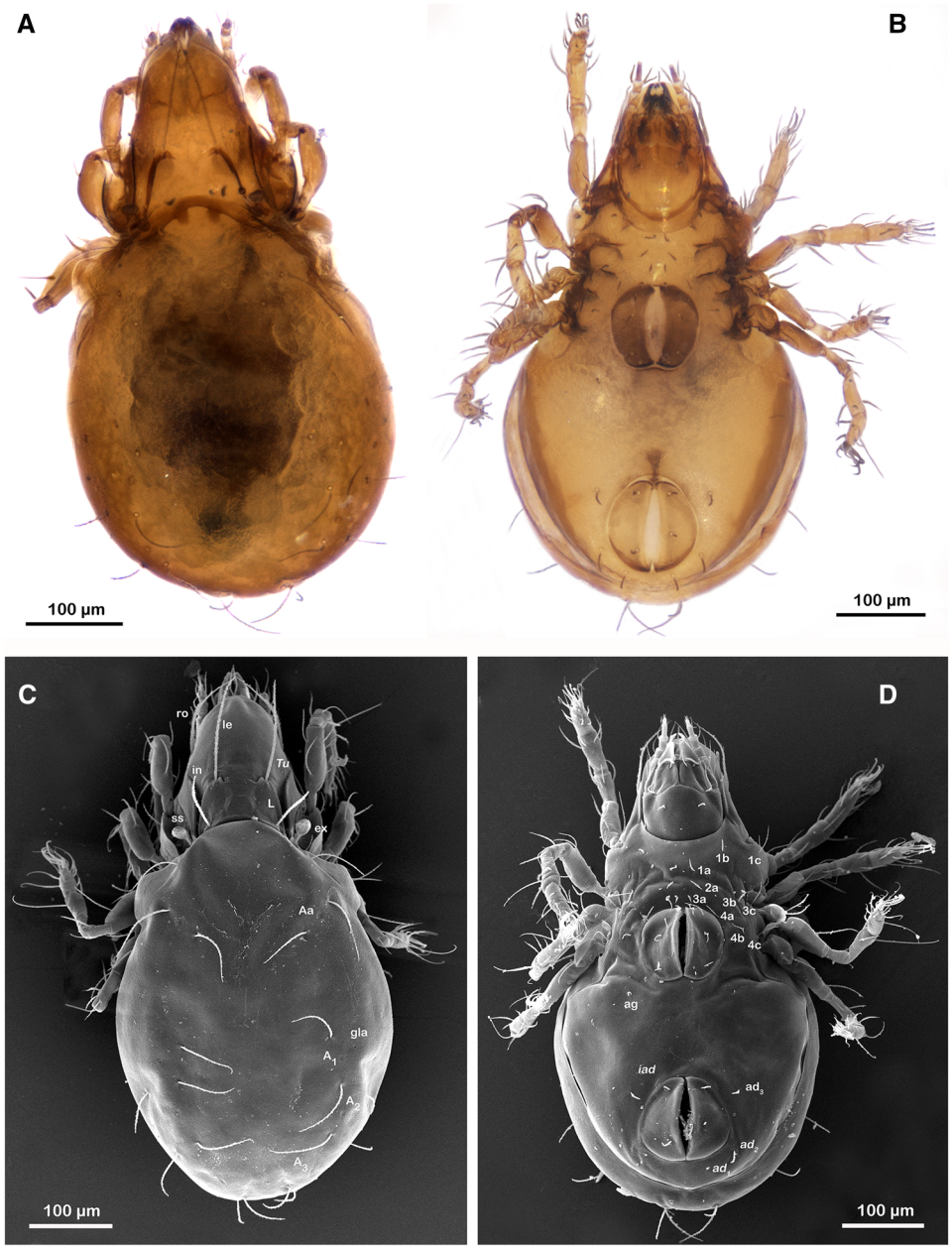


Figure 5 *Maudheimia petronia*. Light microscopy: dorsal view (A) and ventral view (B); and scanning electron microscopy: dorsal view (C) and ventral view (D) with epimeral setae in their correct setal formula: 3-1-3-3. Abbreviations: Aa, A_1, A_2, A_3, octotaxic porous areas; ad_1, ad_2, ad_3, adanal setae; *ag*, aggenital setae; *ex*, exobothridial setae; *gla*, opening of opisthonotal gland; *iad*, adanal lyrifissures; *in*, interlamellar setae; *L*, lamella; *le*, lamellar setae; *ro*, rostral setae; *ss*, sensillum; *Tu*, tutorium.

Morphology

All specimens (both sexes) show little variation in dimensions without evident differences between the two sexes, with measurements between 560 and 610 µm (Figs 5, 6). Consistent with the original description, analysed samples show body surface and leg cuticle weakly sclerotized, brown in colour (Figs 5A–B, 6A), with a reduced presence of waxy cerotegument, which is often more visible around the insertion of the legs (Fig. 6B). A fine network of small tubercles characterizes the microsculpture, which is more evident on the dorsal part of the notogaster.

Prodorsum

Rostrum rounded, with rostral setae (*ro*) ~ 100 µm long, unilaterally barbed, laterally inserted far back from the anterior margin of the rostrum. Owing to their curved shape, the setae follow the contour of the prodorsum, with their tips extending beyond the anterior margin of the rostrum (Fig. 5C).

Short lamellae (*L*), in the form of convergent ridges, follow anteriorly to the pseudostigmata, extending anteromedially for less than half the length of the prodorsum. Along their course, they widen and, approaching the apex, curve medially, bearing a notch that creates a hint of two small cusps,

Downloaded from academic.oup.com/zoolinnean/article/208/2/zlag163/9003135 by Università degli studi di Siena user on 28 October 2026

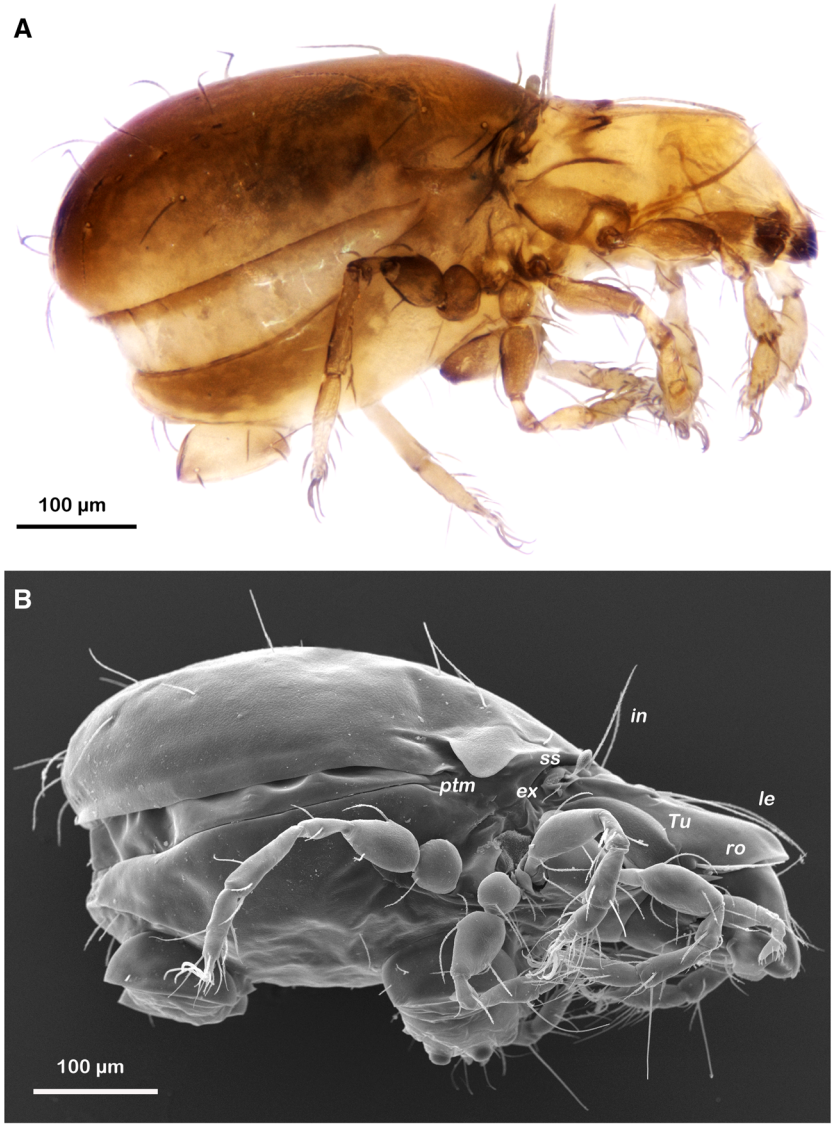


Figure 6 *Maudheimia petronia.* Light microscopy: (A) lateral view; Scanning electron microscopy (SEM): (B) lateral view, (*ro*) = rostral setae, (*le*) = lamellar setae, (*in*) = interlamellar setae, (*Tu*) = tutorium, (*ptm*) = pteromorph, (*ex*) = exobothridial setae, (*ss*) = sensillum.

into which the lamellar setae (*le*) are inserted. The medial cusp extends posteromedially, tapering to a short, thin point. Consistent with the original description (Wallwork 1962) and with Coetzee's subsequent revision (1997), the translamella does not appear to be present in all individuals and when present it appears as a thin edge that is difficult to interpret under the optical microscope; in contrast, a thin translamella is identified by scanning electron microscopy (SEM), although it sometimes does not develop completely. Lamellar setae (*le*) and interlamellar setae (*in*) are present, the former longer (115–120 µm long) than the latter (60–70 µm long). Lamellar setae are thick structures that are smooth in their first proximal third and extensively barbed over the entire surface of the remaining part that ends close to the rostral edge, sometimes exceeding it. Interlamellar setae are thinner in appearance than the lamellar setae and also barbed along the entire surface, with the apex approaching or slightly exceeding the insertion point of the lamellar setae. A short, finely barbed exobothridial seta (*ex*), measuring 25–30 µm, emerges from the cuticle laterally to the sensillum (*ss*) (Figs 5C, 6B).

Each cup-shaped bothridium is partly covered by the anterior margin of the notogaster. Its dorsoventrally flattened orifice opens upwards, anterolaterally, and gives rise to a sensillum with a short stalk and a globose/clavate, finely barbed head (Figs 5C, 6B).

Laterally, the tutorium (*Tu*) can be seen in the typical shape described for *M. petronia*. It appears as a short smooth, narrow, sclerotized, and arched ridge, with the proximal part touching a large pedotectum I and distal apex completely tapering near the middle of the lateral surface of the prodorsum (Figs 5C, 6).

Notogaster

Ovoid in shape, with its arched medial anterior margin partly covering the base of the prodorsum. A couple of small, triangular, immovable pteromorphs (*ptm*) are bent ventrally

Downloaded from academic.oup.com/zoolinnean/article/208/2/zlag163/9003135 by Università degli studi di Siena user on 28 October 2026

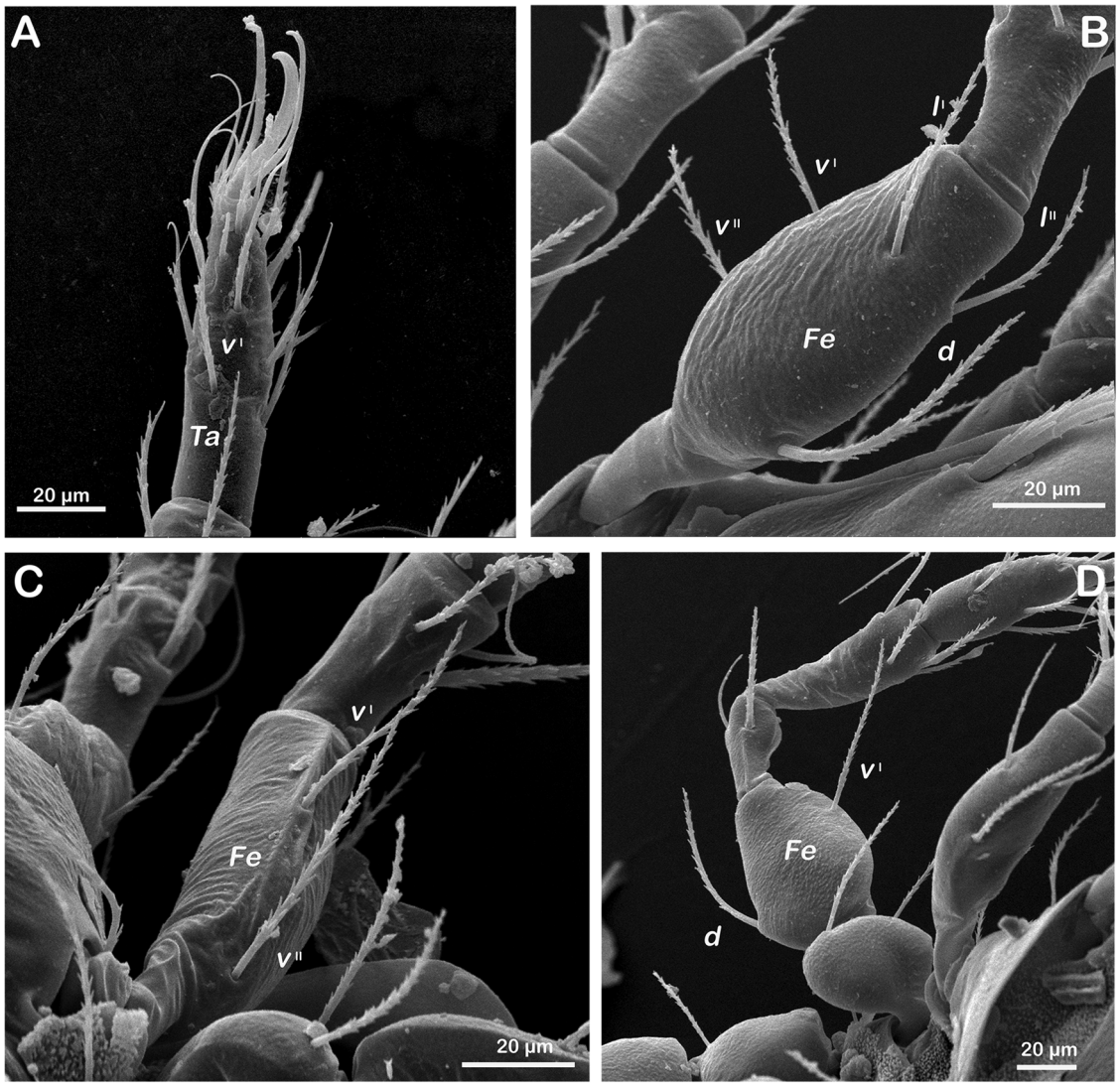


Figure 7 *Maudheimia petronia*. Scanning electron microscopy (SEM): images showing the presence of ventral seta *v′* on tarsus I (*Ta*) (A); femur I (*Fe*) bearing ventral setae *v′* and *v″*, dorsal seta *d*, and lateral setae *l′* and *l″* (B); femur II (*Fe*) bearing ventral setae *v′* and *v″* (C); and femur III (*Fe*) bearing dorsal seta *d* and ventral seta *v′*, with the lateral seta *l′* absent (D).

(Fig. 6B). Ten pairs of thickened notogastral setae are smooth in their proximal portion and distally completely barbed. Their average length is ~60–70 µm, with an arrangement corresponding to that reported by Wallwork (1962) and Coetzee (1997) (Fig. 5A, C). The analysis of the specimens confirms that the arrangement of the octotaxic porous areas agrees with Coetzee's description rather than Wallwork's (Fig. 5C). Lyrifissures (*im*), aligned with the longitudinal body axis, are located anterolaterally to the seta *lp*; posterior to these, the porous area A_1 is visible and, more laterally, the opening of the opisthonotal gland (*gla*) (Fig. 5C). Ventrally, *M. petronia* shows a smooth surface, with short, incomplete apodemes; all ventral setae of medium length are strongly barbed. The structures present in the ventral region are congruent with previous descriptions. Noteworthy is the presence, posteriorly to pedotectum II, of epimeral seta *3c*, confirming the epimeral setal formula (3-1-3-3) proposed by Coetzee (1997) (Fig. 5B, D).

Genital plates, rounded anteriorly, have six pairs of barbed genital setae, and a pair of aggenital setae (*ag*) is posterolateral to the genital aperture. Sexual dimorphism seems to be related to the shape of the genital plates, which are narrower posteriorly in males, more rounded and larger in females (Fig. 5B, D).

The anal aperture, strongly rounded in shape, bears anal plates with two pairs of setae. It is surrounded anterolaterally by a pair of short adanal lyrifissures (*iad*) and, posteriorly, by three pairs of adanal setae (ad_1, ad_2, and ad_3). Like all the setae of the ventral region, those of the anal region are also barbed (Fig. 5B, D).

Legs

All tarsi are tridactyl, with a shorter and more curved median claw, but slightly more robust than the lateral ones. All setae are strongly barbed. Specifically, we investigated the chaetotaxic inconsistency reported by Coetzee (1997) for *M. petronia* and *M. wilsoni* regarding the variable presence of the ventral seta (*v′*) on tarsus I and femora I–II and the lateral seta (*l′*) on femur III. Our analyses of specimens from the three localities, using both light microscopy and SEM, confirmed

Downloaded from academic.oup.com/zoolinnean/article/208/2/zlag163/9003135 by Università degli studi di Siena user on 28 October 2026

pronounced variability in these characters; in several individuals, this variability also exhibits asymmetry (i.e. occurring on one only side of the body). However, when present, the ventral setae (*v′*) on tarsus I, femur I, and femur II conformed to the arrangement described by Coetzee (1997), as illustrated in Fig. 7A–C. In contrast, the lateral seta (*l′*) on femur III was consistently absent in all examined specimens (Figs 6B, 7D).

Discussion

The integrated morphological and mitogenomic analyses of *M. petronia* presented in this study provide new insights into the evolutionary history, biogeography, and molecular peculiarities of Antarctic Oribatida. The main findings are discussed below in thematic sections, each addressing a specific aspect of these results.

Mitochondrial gene order, architecture, and structural constraints

As for the comparative analyses of Brachypylina mtDNA gene order, the CREx reconstructions identified multiple rearrangement events across the analysed genomes. In this respect, rearrangement distances [low values (0–1) denote highly conserved gene orders, whereas higher values ($\geq$4–5) reflect more derived or divergent mitogenomic architectures] were lowest between *M. petronia* and *C. pusillus* and generally remained low among *M. petronia*, *C. imperatoria*, *E. contaminatus*, and *Oribatula* sp., indicating a relatively conserved mitochondrial genomic architecture within this group. In contrast, *O. sakamorii* exhibits substantially higher distances relative to the remaining taxa, suggesting a more derived gene order configuration. Most differences can be explained by transpositions (T) and tandem duplication–random loss (TDRL) events, whereas inversions (I) and inverted transpositions (iT) are less common (Supplementary Table S3). The TDRL processes primarily affected tRNA genes (especially *trnL1*, *trnL2*, *trnE*, and *trnS1*), identifying these regions as recurrent hotspots of mitochondrial rearrangement. These localized duplications and subsequent random losses provide a plausible mechanism for the observed differences in gene order among the analysed brachypyline taxa.

Overall, the pattern of rearrangements suggests a gradual mode of mitochondrial genome evolution, characterized by successive small-scale transpositions and duplications that reshaped gene order without major disruption of the overall genomic architecture. Notably, all taxa apart from *C. pusillus* and *M. petronia* exhibit distinct mitotypes, consistent with the extensive variability in gene order frequently observed within Trombidiformes and Acariformes, even among congeneric species.

In animals, mitochondrial tRNAs typically adopt a cloverleaf secondary structure consisting of four arms: the aminoacyl (AA) arm, D arm, anticodon (AC) arm, and T arm. A well-known exception is the serine tRNA with the GCT anticodon, which lacks the D arm in nearly all metazoans and is considered an ancestral character state in this lineage (Masta and Boore 2008). Although losses of individual arms are generally rare in animals, several arthropod and nematode lineages deviate markedly from this canonical configuration (see next section). The mitochondrial genome of *M. petronia* falls within the size range typical of Acariformes and retains the complete complement of 37 genes, including all PCGs and tRNAs. Relative to the M42 ground pattern (Aydemir 2024), only a single rearrangement involving the transposition of *trnE* was detected. In Brachypylina, most mitochondrial gene-order differences involve tRNA genes, whereas the arrangement of PCGs appears comparatively stable, a pattern also observed in other Acariformes lineages (Arribas *et al.* 2020). Despite this conserved gene order, the mitochondrial genome of *M. petronia* exhibits pronounced genomic compaction, as indicated by the high frequency of gene overlaps, including overlaps between genes encoded on the same strand. Such compact organization parallels patterns reported in other arachnids and is generally interpreted as the result of strong directional selection favouring reduced mitochondrial genome size and enhanced replication efficiency (Boore 1999, Masta and Boore 2004). A seven-nucleotide overlap between *atp8* and *atp6*, frequently observed in arthropod mitogenomes, is likely to reflect bicistronic transcription of these genes. A more unusual feature involves the apparent overlap between the 3′ end of *nad3* and the 5′ end of *trnA*, which spans the full length of the annotated *trnA* sequence despite both genes being encoded on the same strand. A canonical stop codon for *nad3* occurs two nucleotides downstream of the annotated *trnA* boundary, suggesting non-standard transcript processing. Several scenarios might account for this pattern, including alternative termination of *nad3*, atypical cleavage of polycistronic transcripts, or the presence of a highly modified or vestigial tRNA gene. Comparable cases in mtDNA of other metazoans indicate that remnants of tRNA-like structures can persist as processing signals rather than as fully functional genes (Dörner *et al.* 2001). Based on the conserved adjacency of *nad3* and *trnA* in ancestral arthropod and acarine gene-order models (Xue *et al.* 2016), the predominance of acarine gene orders retaining this arrangement and the consistent adjacency of *trnW* and *trnC* within Oribatida (Aydemir 2024), *trnA* in *M. petronia* most probably resides between *nad3* and *trnL2*. The extreme truncation of mitochondrial tRNAs observed in *M. petronia* is consistent with the condition widely reported in Acariformes mites (including Sarcoptiformes and Trombidiformes), which frequently exhibit extensive loss of canonical secondary structural elements, and contrasts with the comparatively more conserved cloverleaf tRNA structures typically found in Parasitiformes (Xue *et al.* 2016, Yang *et al.* 2022). This pattern might reflect that structural degeneration, rather than consistent reductions in tRNA gene length, represents the primary mode of tRNA evolution in these lineages.

Extensive mitochondrial tRNA truncation and compensatory evolution

Within its highly compact mitochondrial genome, the most distinctive feature of *M. petronia* is the extensive reduction of mitochondrial tRNA structure. Animal mitochondrial tRNAs typically range from 70 to 100 nucleotides in length, whereas markedly shortened and even armless tRNAs have

Downloaded from academic.oup.com/zoolinnean/article/208/2/zlag163/9003135 by Università degli studi di Siena user on 28 October 2026

been reported only in a limited number of metazoan lineages (Wolstenholme *et al.* 1987, Chen *et al.* 2011, Ozerova *et al.* 2024, Ye *et al.* 2025). Among these, enoplean nematodes represent one of the best-characterized examples, possessing multiple mitochondrial tRNAs lacking both D and T arms (Jühling *et al.* 2012, Wende *et al.* 2014, Schäffer *et al.* 2018).

In *M. petronia*, the loss of one or both arms, together with frequent mismatches in stem regions, exceeds the degree of reduction reported for most Acariformes mites (Domes *et al.* 2008, Xue *et al.* 2016). The occurrence of tRNAs completely lacking both arms (e.g. tRNA C) places this species among the most structurally modified mitochondrial tRNA systems known in metazoans, comparable to only a few nematode and tetranychid mite lineages (Wolstenholme *et al.* 1987, Warren and Sloan 2021).

A reductive event affecting tRNA C, tRNA F, and tRNA H has previously been inferred for the common ancestor of Acariformes (Xue *et al.* 2016), but the more extensive modifications observed in *M. petronia* are likely to represent a lineage-specific intensification of this evolutionary trend. Similar episodes of independent tRNA reduction have evolved in several invertebrate groups, particularly nematodes and arachnids, suggesting an unusual tolerance for departures from the canonical cloverleaf structure (Masta and Boore 2008, Jühling *et al.* 2012, Wende *et al.* 2014).

The persistence of such highly reduced tRNAs implies the evolution of compensatory mechanisms that maintain translational functionality. Proposed mechanisms include modifications of mitochondrial ribosomal architecture, altered elongation-factor interactions, RNA-editing processes that restore pairing in destabilized stems, and post-transcriptional maturation pathways that compensate for truncated acceptor arms prior to CCA-tail addition (Yokobori and Pääbo 1995, Börner *et al.* 1996, Warren and Sloan 2021).

Recent transcriptomic studies further indicate that unconventional transcriptional strategies might contribute to tRNA functionality in compact mitochondrial genomes. In the sarcoptiform mite *Tetranychus urticae*, paired sense and antisense expression of several mitochondrial tRNAs has been demonstrated, challenging the traditional view of strictly unidirectional transcription (Warren and Sloan 2021). Such patterns might represent an additional consequence of genome compaction, which is typically associated with reduced intergenic regions and extensive gene overlap (Boore 1999, Lavrov 2007).

In this context, the ambiguous placement of *trnA* in *M. petronia* is particularly noteworthy. Although complete gene loss followed by nuclear encoding and mitochondrial import cannot be excluded, the presence of a plausible secondary structure within the expected genomic interval and the conservation of this locus across Acariformes strongly suggest that *trnA* has been retained in a highly modified form.

Overall, the mitochondrial genome of *M. petronia* provides evidence for a substantially remodelled translational system, probably shaped by genome compaction together with the evolution of compensatory mechanisms acting at the levels of transcription, RNA processing, and translation.

Phylogenetic implications and placement of *Maudheimia*

Phylogenetic analyses based on mitochondrial PCGs recovered topologies consistent with major morphological hypotheses concerning Sarcoptiformes relationships, including the monophyly of Astigmata and Oribatida, with the exception of *S. magnus*, suggesting that astigmatid mites originated within oribatid mites. This latter placement is, nonetheless, consistent with current understanding of oribatid phylogeny (Norton 1998, Lindquist *et al.* 2009, Schatz *et al.* 2011, Behan-Pelletier and Lindo 2023); it was also observed in a previous mtDNA-based phylogenetic study (Li and Xue 2019) and aligns with the traditional separation of Sarcoptiformes into the two cohorts Mixonomatides and Desmonomatides. The former includes the Phthiracaroidea, whereas the latter encompasses all other Sarcoptiform lineages, further divided into the subcohorts Nothrina, Brachypylina, and Astigmata (Fig. 4). Our findings are also broadly congruent with the large-scale molecular analysis by Cordes *et al.* (2024), who demonstrated extensive paraphyly and polyphyly among higher oribatid taxa using 18S rDNA data from >300 species. Their study showed that only a minority of currently recognized superfamilies were consistently recovered as monophyletic, suggesting that convergent evolution has strongly influenced many morphological traits traditionally used in oribatid systematics. The non-monophyly of Ceratozetoidea recovered in our mitogenomic analyses, owing to the placement of *E. contaminatus* within the clade, is consistent with this broader pattern and further supports the need for integrative systematic revisions combining morphology and molecular datasets.

From a morphological perspective, the relationship between oribatid and astigmatid mites has long been debated. These results reinforce the view that Phthiracaroidea represent a deep lineage within Oribatida. The recovery of Astigmata within a paraphyletic Oribatida is likewise consistent with several previous molecular studies (Dabert *et al.* 2010, Li and Xue 2019), although alternative topologies based on different nuclear datasets have also been proposed (Pepato *et al.* 2010, Schäffer *et al.* 2010, Xue *et al.* 2016). Together with the observations by Cordes *et al.* (2024), the present results indicate that acariform mites are likely to be characterized by repeated morphological convergence and the persistence of plesiomorphic character combinations, complicating morphology-based reconstructions.

Within Oribatida, genus *Maudheimia* was consistently placed among the Brachypylina, in agreement with previous morphological revisions (Coetzee 1997, Coetzee and Weigmann 2012). Its close mitochondrial affinities to *Chamobates* and *Ceratozetella* reflect shared aspects of gene order and support the stable placement of Maudheimiidae within Ceratozetoidea (with Phenopelopoidea nested within). However, the instability and non-monophyly observed for several brachypyline lineages in both our analyses and those of Cordes *et al.* (2024) suggest that the current circumscription of Ceratozetoidea might require reassessment in future studies based on broader phylogenomic datasets.

Downloaded from academic.oup.com/zoolinnean/article/208/2/zlag163/9003135 by Università degli studi di Siena user on 28 October 2026

Although the present study was not designed to perform formal molecular dating analyses, the mitogenomic and phylogenetic evidence obtained here contributes to a more robust understanding of the placement of Maudheimiidae within Oribatida. In particular, the consistent recovery of *M. petronia* within Brachypylina and its affinities with ceratozetoid lineages provide independent molecular support for previous morphology-based classifications (Coetzee 1997, Coetzee and Weigmann 2012).

Nevertheless, the present data do not provide a basis for robust inferences regarding the age of Maudheimiidae, the timing of diversification within the genus, or the historical processes underlying its present-day Antarctic distribution. The present mitochondrial dataset includes only a single representative species of the family and lacks the broader taxonomic sampling, nuclear markers, and calibration framework required for reliable temporal and biogeographical reconstruction. Consequently, previous hypotheses concerning the origin and historical persistence of *Maudheimia* in Antarctica (Marshall and Coetzee 2000, Pugh and Convey 2008) cannot be evaluated directly using the present data.

Population structure and historical biogeography

The three Victoria Land populations examined here show low to moderate genetic diversity and a clear pattern of geographically isolated haplogroups. This genetic structure is consistent with the life-history traits of Antarctic soil arthropods, which typically exhibit limited dispersal and long-term population persistence in microrefugia (Stevens and Hogg 2006, Brunetti *et al.* 2021). The absence of deep genetic breaks between populations indicates that *M. petronia* represents a single, evolutionarily coherent species across the sampled region. This pattern aligns with a scenario of small, stable, and geographically isolated populations derived from refugial lineages that survived Pleistocene glacial maxima (Marshall and Coetzee 2000, Collins *et al.* 2023).

One notable exception to this general pattern is observed in the Crater Cirque population, which shows unexpectedly high haplotypic divergence, with intrapopulation *p*-distances exceeding those observed between populations. This pattern suggests a complex demographic history and might reflect the long-term persistence of multiple mitochondrial lineages within a single refugial area. Additional populations and/or nuclear markers will be necessary to distinguish between these hypotheses. The limited number of analysed populations prevents any robust conclusions regarding the role of major geographical barriers in the region (e.g. glaciers and mountain ridges) in shaping the distribution of *M. petronia* specimens. Moreover, different glacier systems might have acted as barriers to dispersal to varying degrees and at different times during the Quaternary, resulting in a spatially and temporally dynamic influence on population connectivity, as suggested for other Antarctic terrestrial invertebrate taxa (Boschi *et al.* 2025).

Morphological stability and taxonomic consistency

Morphological observations under light microscopy and SEM fully corroborate the diagnostic features of *M. petronia*. Characters such as notogastral architecture, porose area patterning, epimeral setation, and cerotegumental structures consistently matched the species diagnosis and exhibited negligible variation across populations. This morphological uniformity is congruent with the genetic data and suggests strong stabilizing selection on phenotypic traits, with reduced developmental plasticity. Such patterns are commonly observed in oribatids from extreme environments, where ecological variability is limited and developmental processes tend to produce highly buffered (canalized) phenotypes (Coetzee 1997). Despite the complete lack of shared haplotypes between the three localities and the clear genetic separation of Crater Cirque (Fig. 1), the morphology of *M. petronia* seems to remain remarkably conserved (morphostasis). The variability found in leg chaetotaxy is not correlated with the identified genetic groups, suggesting that these morphological fluctuations are an expression of phenotypic plasticity rather than ongoing evolutionary divergence. These data support the hypothesis of a strong selective control exerted by the extreme conditions of Victoria Land (Collins *et al.* 2023), which stabilizes the phenotype despite the millennia-long isolation of *M. petronia* populations. Physiological resilience and evolutionary persistence in *Maudheimia* specimens might be linked to their weakly sclerotized exoskeleton and lichen-based diet. The analysed material shows a lightly sclerotized, brown cuticle on the body and legs, accompanied by a sparsely developed waxy cerotegument. A flexible cuticle represents a specialized adaptation to the cold, arid environments of Antarctica, potentially enhancing the ability to maintain contact with moist microhabitats (such as rock crevices, mosses, or lichens) and aiding in water conservation in desiccating conditions. Moreover, in nutrient-poor and low-oxygen environments, where metabolic rates are naturally reduced, investment in a thick, heavily sclerotized exoskeleton might be unnecessary or even disadvantageous. In such systems, morphological traits are expected to be shaped predominantly by abiotic constraints and energy limitation rather than by complex biotic interactions, consistent with the strongly environmentally driven structure of Antarctic terrestrial ecosystems (Convey *et al.* 2014, Chown and Convey 2016).

Conclusion

Overall, this study substantially advances the understanding of *M. petronia* systematics and contributes to a broader knowledge of mtDNA evolution and biogeography in Antarctic Oribatida. Although the presence of *M. petronia* in this sector of the Antarctic continent (where it is endemic) has long been recognized, the present analyses provide an integrated reassessment of its morphology, phylogenetic placement, and

Downloaded from academic.oup.com/zoolinnean/article/208/2/zlag163/9003135 by Università degli studi di Siena user on 28 October 2026

mitochondrial genomic architecture. Morphological evidence confirms that *M. petronia* is fully congruent with the diagnostic characters defined in Wallwork's original description (Wallwork 1962) and in subsequent revisions of the genus by Coetzee (1997) and Coetzee and Weigmann (2012).

At the mitochondrial genomic level, *M. petronia* is characterized by a striking combination of relatively conserved mitochondrial PCG order and extremely derived tRNA structures. The pronounced reduction and structural modification of tRNAs, together with extensive genome compaction, are consistent with evolutionary pressures favouring mitochondrial genome minimization, potentially reducing the costs associated with genome replication and maintenance, although mutational biases and other non-adaptive processes might also contribute to these patterns (Lynch *et al.* 2006, Lynch and Marinov 2015). Despite this extreme structural simplification, populations of *M. petronia* remain genetically cohesive, albeit spatially fragmented, a pattern consistent with long-term persistence in isolated Pleistocene refugia.

Taken together, the principal findings of this study can be summarized as follows: (i) *M. petronia* exhibits highly derived and functionally reduced tRNA structures; (ii) extensive genome compaction and tRNA reduction are likely to represent adaptive features linked to mitochondrial efficiency (although no specific analysis has been performed to test this hypothesis); (iii) the placement of *Maudheimia* within Ceratozetoidea is strongly supported by congruent morphological and mitogenomic evidence; and (iv) contemporary populations of *M. petronia* form a genetically cohesive yet geographically fragmented species shaped by historical isolation. Future research should prioritize mitochondrial transcriptomic analyses (RNA sequencing) and functional assays of tRNA processing to elucidate how these highly reduced tRNAs remain operational within the mitochondrial translational machinery.

Expanded phylogenomic datasets integrating nuclear markers, complete sampling of all described *Maudheimia* species, and time-calibrated analyses will be essential to determine whether the evolutionary origin of Maudheimiidae pre-dates the final break-up of Gondwana or instead reflects a later Antarctic diversification associated with Neogene and Quaternary climatic oscillations. In parallel, expanded population-genetics and phylogenetic investigations incorporating the remaining *Maudheimia* species would greatly refine our understanding of the evolutionary history and biogeographical diversification of this enigmatic Antarctic mite lineage.

Acknowledgements

We thank Dr Rebecca Pettini for assistance with PCR experiments, and Professor Davide Badano and Professor Pietro Lupetti for technical assistance on optical microscopy and SEM imaging analyses, respectively.

Supplementary material

Supplementary material is available at *Zoological Journal of the Linnean Society* online.

Conflicts of interest

The authors declare no conflicts of interest.

Funding

This research was supported by the Programma Nazionale di Ricerche in Antartide (PNRA; grant PNRA16_00234 to A.C.) and by the National Biodiversity Future Center (NBFC), with funding to the University of Siena, Department of Life Sciences, from the Italian Ministry of University and Research under the National Recovery and Resilience Plan (PNRR), Mission 4, Component 2, Investment 1.4, project CN00000033.

Data availability

All data are incorporated into the article and its online Supplementary material. The mitochondrial genome sequence of *Maudheimia petronia* is available in GenBank (https://www.ncbi.nlm.nih.gov/nuccore/) under accession number PX633171, and the *cox1* haplotype sequences are available under accession numbers PX498765–PX498782. Raw sequencing reads are available in the NCBI Sequence Read Archive (https://www.ncbi.nlm.nih.gov/sra/) under accession number SRP289641, associated with BioProject PRJNA673074 and BioSample SAMN16587686 (sample name: Pool1). Additional supporting data are provided in the article and its online supplementary material.

References

Al Arab M, Höner Zu Siederdissen C, Tout K *et al.* Accurate annotation of protein-coding genes in mitochondrial genomes. *Molecular Phylogenetics and Evolution* 2017;**106**:209–16. https://doi.org/10.1016/j.ympev.2016.09.024

Arribas P, Andújar C, Moraza ML *et al.* Mitochondrial metagenomics reveals the ancient origin and phylodiversity of soil mites and provides a phylogeny of the Acari. *Molecular Biology and Evolution* 2020;**37**:683–94. https://doi.org/10.1093/molbev/msz255

Aydemir HB. Quantification of rearrangements and evolution of mitochondrial gene order of Acari (Chelicerata: Arachnida). *Parasitology Research* 2024;**123**:389. https://doi.org/10.1007/s00436-024-08416-6

Balogh J, Balogh P. A review of the Oribatuloidea Thor, 1929 (Acari: Oribatei). *Acta Zoologica Academiae Scientiarum Hungaricae* 1984;**30**:257–313.

Balogh J, Balogh P. *The Oribatid Mite Genera of the World*, Volumes **1 and 2**. Budapest: Hungarian Natural History Museum, 1992. ISBN 9637093044.

Behan-Pelletier V, Lindo Z. *Oribatid Mites: Biodiversity, Taxonomy and Ecology*. Boca Raton, FL: CRC Press, 2023. https://doi.org/10.1201/9781003214649

Bernt M, Merkle D, Ramsch K *et al.* CREx: inferring genomic rearrangements based on common intervals. *Bioinformatics (Oxford, England)* 2007;**23**:2957–8. https://doi.org/10.1093/bioinformatics/btm468

Downloaded from academic.oup.com/zoolinnean/article/208/2/zlag163/9003135 by Università degli studi di Siena user on 28 October 2026

Bigg EK. The supercooling of water. *Proceedings of the Physical Society. Section B* 1953;**66**:688–94. https://doi.org/10.1088/0370-1301/66/8/309

Block W, Convey P. The biology, life cycle and ecophysiology of the Antarctic mite *Alaskozetes antarcticus*. *Journal of Zoology* 1995;**236**:431–49. https://doi.org/10.1111/j.1469-7998.1995.tb02723.x

Block W, Young SR. Measurement of supercooling in small arthropods and water droplets. *CryoLetters* 1979;**1**:85–91.

Boore JL. Animal mitochondrial genomes. *Nucleic Acids Research* 1999;**27**:1767–80. https://doi.org/10.1093/nar/27.8.1767

Börner GV, Mörl M, Janke A *et al.* RNA editing changes the identity of a mitochondrial tRNA in marsupials. *The EMBO Journal* 1996;**15**:5949–57.

Boschi S, Cucini C, Cardaioli E *et al.* Population genetics and the role of dispersal barriers in the Antarctic springtail *Kaylathalia klovstadi* (Collembola, Isotomidae). *Journal of Zoology* 2025;**326**:109–20. https://doi.org/10.1111/jzo.70012

Brunetti C, Siepel H, Convey P *et al.* Overlooked species diversity and distribution in the Antarctic mite genus *Stereotydeus*. *Diversity* 2021;**13**:506. https://doi.org/10.3390/d13100506

Carapelli A, Brunetti C, Cucini C *et al.* The mitogenome of the true bug *Nysius cymoides* (Insecta, Heteroptera) and the phylogeny of Lygaeoidea. *Mitochondrial DNA. Part B, Resources* 2021;**6**:2366–8. https://doi.org/10.1080/23802359.2021.1951139

Carapelli A, Greenslade P, Nardi F *et al.* Evidence for cryptic diversity in the "pan-Antarctic" springtail *Friesea antarctica* and the description of two new species. *Insects* 2020;**11**:141. https://doi.org/10.3390/insects11030141

Chen WJ, Bu Y, Carapelli A *et al.* The mitochondrial genome of *Sinentomon erythranum* (Arthropoda: Hexapoda: Protura): an example of highly divergent evolution. *BMC Evolutionary Biology* 2011;**11**:246. https://doi.org/10.1186/1471-2148-11-246

Chown SL, Convey P. Antarctic entomology. *Annual Review of Entomology* 2016;**61**:119–37. https://doi.org/10.1146/annurev-ento-010715-023537

Clayton DA. Transcription and replication of animal mitochondrial DNAs. *International Review of Cytology* 1992;**141**:217–32. https://doi.org/10.1016/s0074-7696(08)62067-7

Coetzee L. The Antarctic mite genus *Maudheimia* (Acari, Oribatida). *Navorsinge Van Die Nasionale Museum, Bloemfontein* 1997;**13**:101–35.

Coetzee L, Weigmann G. Systematic revision of the genus *Maudheimia* Dalenius, 1958 (Acari: Oribatida). *Zootaxa* 2012;**3295**:65–8. https://doi.org/10.11646/zootaxa.3295.1.4

Collins GE, Hogg ID, Convey P *et al.* Spatial and temporal scales matter when assessing the species and genetic diversity of springtails (Collembola) in Antarctica. *Frontiers in Ecology and Evolution* 2019;**7**:76. https://doi.org/10.3389/fevo.2019.00076

Collins GE, Hogg ID, Convey P *et al.* Genetic diversity of soil invertebrates corroborates timing estimates for past collapses of the West Antarctic Ice Sheet. *Proceedings of the National Academy of Sciences of the United States of America* 2020;**117**:22293–302. https://doi.org/10.1073/pnas.2007925117

Collins GE, Young MR, Convey P *et al.* Biogeography and genetic diversity of terrestrial mites in the Ross Sea region, Antarctica. *Genes* 2023;**14**:606. https://doi.org/10.3390/genes14030606

Convey P, Biersma EM, Casanova-Katny A *et al.* Refuges of Antarctic diversity. In: Oliva M, Ruiz-Fernández J (eds.), *Past Antarctica: Paleoclimatology and Climate Change*. London: Academic Press, 2020, 181–200. https://doi.org/10.1016/B978-0-12-817925-3.00010-0

Convey P, Chown SL, Clarke A *et al.* The spatial structure of Antarctic biodiversity. *Ecological Monographs* 2014;**84**:203–44. https://doi.org/10.1890/12-2216.1

Convey P, Gibson JA, Hillenbrand CD *et al.* Antarctic terrestrial life – challenging the history of the frozen continent? *Biological Reviews of the Cambridge Philosophical Society* 2008;**83**:103–17. https://doi.org/10.1111/j.1469-185X.2008.00034.x

Convey P, Stevens MI. Antarctic biodiversity. *Science* 2007;**317**:1877–8. https://doi.org/10.1126/science.1147261

Cordes P, Pan X, Murvanidze M *et al.* Convergent evolution revealed by paraphyly and polyphyly of many taxa of oribatid mites: a molecular approach. *Experimental & Applied Acarology* 2024;**93**:787–802. https://doi.org/10.1007/s10493-024-00960-1

Cucini C, Carapelli A, Brunetti C *et al.* Characterization of the complete mitochondrial genome of *Neoasterolepisma foreli* (Insecta: Zygentoma: Lepismatidae) and the phylogeny of basal Ectognatha. *Mitochondrial DNA. Part B, Resources* 2021a;**6**:119–21. https://doi.org/10.1080/23802359.2020.1848480

Cucini C, Fanciulli PP, Frati F *et al.* Re-evaluating the internal phylogenetic relationships of Collembola by means of mitogenome data. *Genes* 2021b;**12**:44. https://doi.org/10.3390/genes12010044

Cucini C, Nardi F, Magnoni L *et al.* Microhabitats, macro-differences: a survey of temperature records in Victoria Land terrestrial and freshwater environments. *Antarctic Science* 2022;**34**:256–65. https://doi.org/10.1017/S0954102022000050

Cucini C, Pons J, Funari R *et al.* EZmito2: a tool suite for mitochondrial genome dataset preparation, population genetics, and visualization. *Molecular Biology and Evolution* 2026;**43**:msag210. https://doi.org/10.1093/molbev/msag210

Dabert M, Witalinski W, Kazmierski A *et al.* Molecular phylogeny of acariform mites (Acari, Arachnida): strong conflict between phylogenetic signal and long-branch attraction artifacts. *Molecular Phylogenetics and Evolution* 2010;**56**:222–41. https://doi.org/10.1016/j.ympev.2009.12.020

Dalenius P, Wilson O. On the soil fauna of the Antarctic and of the Sub-Antarctic islands. The Oribatidae (Acari). *Arkiv för Zoologi* 1958;**11**:393–425.

Darty K, Denise A, Ponty Y. VARNA: interactive drawing and editing of the RNA secondary structure. *Bioinformatics*

Downloaded from academic.oup.com/zoolinnean/article/208/2/zlag163/9003135 by Università degli studi di Siena user on 28 October 2026

(Oxford, England) 2009;**25**:1974–5. https://doi.org/10.1093/bioinformatics/btp250

Dierckxsens N, Mardulyn P, Smits G. NOVOPlasty: *de novo* assembly of organelle genomes from whole genome data. *Nucleic Acids Research* 2017;**45**:e18. https://doi.org/10.1093/nar/gkw955

Domes K, Maraun M, Scheu S *et al.* The complete mitochondrial genome of the sexual oribatid mite *Steganacarus magnus*: genome rearrangements and loss of tRNAs. *BMC Genomics* 2008;**9**:532. https://doi.org/10.1186/1471-2164-9-532

Donath A, Jühling F, Al-Arab M *et al.* Improved annotation of protein-coding gene boundaries in metazoan mitochondrial genomes. *Nucleic Acids Research* 2019;**47**:10543–52. https://doi.org/10.1093/nar/gkz833

Dörner M, Altmann M, Pääbo S *et al.* Evidence for import of a lysyl-tRNA into marsupial mitochondria. *Molecular Biology of the Cell* 2001;**12**:2688–98. https://doi.org/10.1091/mbc.12.9.2688

Excoffier L, Laval G, Schneider S. Arlequin ver. 3.0: an integrated software package for population genetics data analysis. *Evolutionary Bioinformatics* 2005;**1**:47–50. https://doi.org/10.1177/117693430500100003

Folmer O, Black M, Hoeh W *et al.* DNA primers for amplification of mitochondrial cytochrome *c* oxidase subunit I from diverse metazoan invertebrates. *Molecular Marine Biology and Biotechnology* 1994;**3**:294–9.

Hebert PDN, Cywinska A, Ball SL *et al.* Biological identifications through DNA barcodes. *Proceedings of the Royal Society of London. Series B: Biological Sciences* 2003;**270**:313–21. https://doi.org/10.1098/rspb.2002.2218

Jühling F, Pütz J, Florentz C *et al.* Armless mitochondrial tRNAs in Enoplea (Nematoda). *RNA Biology* 2012;**9**:1161–66. https://doi.org/10.4161/rna.21630

Klimov PB, O'Connor BM. Improved tRNA prediction in the American house dust mite reveals widespread occurrence of extremely short minimal tRNAs in acariform mites. *BMC Genomics* 2009;**10**:598. https://doi.org/10.1186/1471-2164-10-598

Larsson A. AliView: a fast and lightweight alignment viewer and editor for large datasets. *Bioinformatics (Oxford, England)* 2014;**30**:3276–8. https://doi.org/10.1093/bioinformatics/btu531

Laslett D, Canbäck B. ARWEN: a program to detect tRNA genes in metazoan mitochondrial nucleotide sequences. *Bioinformatics (Oxford, England)* 2008;**24**:172–5. https://doi.org/10.1093/bioinformatics/btm573

Lavrov DV. Key transitions in animal evolution: a mitochondrial DNA perspective. *Integrative and Comparative Biology* 2007;**47**:734–43. https://doi.org/10.1093/icb/icm045

Leigh JW, Bryant D. PopART: full-feature software for haplotype network construction. *Methods in Ecology and Evolution* 2015;**6**:1110–6. https://doi.org/10.1111/2041-210X.12410

Li D, Liu CM, Luo R *et al.* MEGAHIT: an ultra-fast single-node solution for large and complex metagenomics assembly via succinct de Bruijn graph. *Bioinformatics (Oxford, England)* 2015;**31**:1674–6. https://doi.org/10.1093/bioinformatics/btv033

Li W-N, Xue X-F. Mitochondrial genome reorganization provides insights into the relationship between oribatid mites and astigmatid mites (Acari: Sarcoptiformes: Oribatida). *Zoological Journal of the Linnean Society* 2019;**187**:585–98. https://doi.org/10.1093/zoolinnean/zlz044

Lindquist EE, Krantz GW, Walter DE. Classification. In: Krantz GW, Walter DE (eds.) *A Manual of Acarology*. Lubbock, TX: Texas Tech University Press, 2009, 97–103.

Lowe TM, Eddy SR. tRNAscan-SE: a program for improved detection of transfer RNA genes in genomic sequence. *Nucleic Acids Research* 1997;**25**:955–64. https://doi.org/10.1093/nar/25.5.0955

Lynch M, Koskella B, Schaack S. Mutation pressure and the evolution of organelle genomic architecture. *Science (New York, N.Y.)* 2006;**311**:1727–30. https://doi.org/10.1126/science.1118884

Lynch M, Marinov GK. The bioenergetic costs of a gene. *Proceedings of the National Academy of Sciences of the United States of America* 2015;**112**:15690–5.

Marshall DJ, Coetzee L. Historical biogeography and ecology of a Continental Antarctic mite genus, *Maudheimia* (Acari, Oribatida): evidence for a Gondwanan origin and Pliocene–Pleistocene speciation. *Zoological Journal of the Linnean Society* 2000;**129**:111–28. https://doi.org/10.1006/zjls.1999.0209

Marshall DJ, Convey P. Compact aggregation and life-history strategy in a continental Antarctic mite. In: Bruin J, van der Geest LPS, Sabelis MW (eds.), *Ecology and Evolution of the Acari*. Dordrecht: Kluwer Academic Publishers, 1999, 557–67. https://doi.org/10.1007/978-94-017-1343-6_47

Masta SE, Boore JL. The complete mitochondrial genome sequence of the spider *Habronattus oregonensis* reveals rearranged and extremely truncated tRNAs. *Molecular Biology and Evolution* 2004;**21**:893–902. https://doi.org/10.1093/molbev/msh096

Masta SE, Boore JL. Parallel evolution of truncated transfer RNA genes in arachnid mitochondrial genomes. *Molecular Biology and Evolution* 2008;**25**:949–59. https://doi.org/10.1093/molbev/msn051

Matsuoka K, Skoglund A, Roth G *et al.* Quantarctica [dataset]. Norwegian Polar Institute, 2018. https://doi.org/10.21334/npolar.2018.8516e961 (30 November 2025, date last accessed).

McGaughran A, Torricelli G, Carapelli A *et al.* Contrasting phylogeographical patterns for springtails reflect different evolutionary histories between the Antarctic Peninsula and continental Antarctica. *Journal of Biogeography* 2010;**37**:103–19. https://doi.org/10.1111/j.1365-2699.2009.02178.x

Mortimer E, Jansen van Vuuren B, Lee JE *et al.* Mite dispersal among the Southern Ocean Islands and Antarctica before the last glacial maximum. *Proceedings of the Royal Society B: Biological Sciences* 2011;**278**:1247–55. https://doi.org/10.1098/rspb.2010.1779

Norton RA. Morphological evidence for the evolutionary origin of Astigmata (Acari: Acariformes). *Experimental & Applied*

Downloaded from academic.oup.com/zoolinnean/article/208/2/zlag163/9003135 by Università degli studi di Siena user on 28 October 2026

Acarology 1998;**22**:559–94. https://doi.org/10.1023/A:1006135509248

Ozerova I, Fallmann J, Mörl M *et al.* Aberrant mitochondrial tRNA genes appear frequently in animal evolution. *Genome Biology and Evolution* 2024;**16**:evae232. https://doi.org/10.1093/gbe/evae232

Pepato AR, da Rocha CE, Dunlop JA. Phylogenetic position of the acariform mites: sensitivity to homology assessment under total evidence. *BMC Evolutionary Biology* 2010;**10**:235. https://doi.org/10.1186/1471-2148-10-235

Podsiadlowski L, Carapelli A, Nardi F *et al.* The mitochondrial genomes of *Campodea fragilis* and *Campodea lubbocki* (Hexapoda: Diplura): high genetic divergence in a morphologically uniform taxon. *Gene* 2006;**381**:49–61. https://doi.org/10.1016/j.gene.2006.06.009

Pugh PJA, Convey P. Surviving out in the cold: Antarctic endemic invertebrates and their refugia. *Journal of Biogeography* 2008;**35**:2176–86. https://doi.org/10.1111/j.1365-2699.2008.01953.x

Rambaut A. FigTree v1.4.4, 2018. Available at: http://tree.bio.ed.ac.uk/software/figtree/ (23 December 2025, date last accessed).

Robinson J, Thorvaldsdóttir H, Winckler W *et al.* Integrative genomics viewer. *Nature Biotechnology* 2011;**29**:24–6. https://doi.org/10.1038/nbt.1754

Ross GM, Rymer PD, Cook JM *et al.* Phylogeography of Antarctic soil invertebrate fauna reveals ancient origins, repeated colonization and recent evolution. *Antarctic Science* 2025;**37**:13–30. https://doi.org/10.1017/S0954102024000403

Schäffer S, Koblmüller S, Klymiuk I *et al.* The mitochondrial genome of the oribatid mite *Paraleius leontonychus*: new insights into tRNA evolution and phylogenetic relationships in acariform mites. *Scientific Reports* 2018;**8**:7558. https://doi.org/10.1038/s41598-018-25981-w

Schäffer S, Koblmüller S, Pfingstl T *et al.* Ancestral state reconstruction reveals multiple independent evolution of diagnostic morphological characters in the "Higher Oribatida" (Acari), conflicting with current classification schemes. *BMC Evolutionary Biology* 2010;**10**:246. https://doi.org/10.1186/1471-2148-10-246

Schatz H, Behan-Pelletier VM, OConnor BM *et al.* Suborder Oribatida van der Hammen, 1968. *Zootaxa* 2011;**3148**:141–8. https://doi.org/10.11646/zootaxa.3148.1.26

Sievers F, Higgins DG. Clustal Omega for making accurate alignments of many protein sequences. *Protein Science* 2018;**27**:135–45. https://doi.org/10.1002/pro.3290

Sømme L, Strømme A, Zachariassen KE. Notes on the ecology and physiology of the Antarctic oribatid mite *Maudheimia wilsoni*. *Polar Research* 1993;**12**:21–5. https://doi.org/10.3402/polar.v12i1.6699

Søvik G. The biology and life history of arctic populations of the littoral mite *Ameronothrus lineatus* (Acari, Oribatida). *Experimental & Applied Acarology* 2004;**34**:3–20. https://doi.org/10.1023/b:appa.0000044436.80588.96

Stevens MI, Greenslade P, Hogg ID *et al.* Southern hemisphere springtails: could any have survived glaciation of Antarctica? *Molecular Biology and Evolution* 2006;**23**:874–82. https://doi.org/10.1093/molbev/msj073

Stevens MI, Hogg ID. Contrasting levels of mitochondrial DNA variability between mites (Penthalodidae) and springtails (Hypogastruridae) from the Trans-Antarctic Mountains suggest long-term effects of glaciation and life history on substitution rates, and speciation processes. *Soil Biology and Biochemistry* 2006;**38**:3171–80. https://doi.org/10.1016/j.soilbio.2006.01.009

Teets NM, Denlinger DL. Surviving in a frozen desert: environmental stress physiology of terrestrial Antarctic arthropods. *The Journal of Experimental Biology* 2014;**217**:84–93. https://doi.org/10.1242/jeb.089490

Terauds A, Lee JR. Antarctic biogeography revisited: updating the Antarctic Conservation Biogeographic Regions. *Diversity and Distributions* 2016;**22**:836–40. https://doi.org/10.1111/ddi.12453

Wallwork JA. Antarctic oribatid mites Maudheimia petronia n. sp. (Acari: Oribatei), an oribatid mite from Antarctica. *Pacific Insects* 1962;**4**:865–68.

Warren JM, Sloan DB. Hopeful monsters: unintended sequencing of famously malformed mite mitochondrial tRNAs reveals widespread expression and processing of sense–antisense pairs. *NAR Genomics and Bioinformatics* 2021;**3**:lqaa111. https://doi.org/10.1093/nargab/lqaa111

Wende S, Platzer M, Jühling F *et al.* Biological evidence for the world's smallest tRNAs. *Biochimie* 2014;**100**:151–8. https://doi.org/10.1016/j.biochi.2013.07.034

Wolstenholme DR, Macfarlane JL, Okimoto R *et al.* Bizarre tRNAs inferred from DNA sequences of mitochondrial genomes of nematode worms. *Proceedings of the National Academy of Sciences of the United States of America* 1987;**84**:1324–8. https://doi.org/10.1073/pnas.84.5.1324

Wong TKF, Ly-Trong N, Ren H *et al.* IQ-TREE 3: phylogenomic inference software using complex evolutionary models. *Molecular Biology and Evolution* 2026;**43**:msag117. https://doi.org/10.1093/molbev/msag117

Xue XF, Guo JF, Dong Y *et al.* Mitochondrial genome evolution and tRNA truncation in Acariformes mites: new evidence from eriophyoid mites. *Scientific Reports* 2016;**6**:18920. https://doi.org/10.1038/srep18920

Yang H, Yang Z, Chen T *et al.* Comparative analysis of tRNA genes in the mitochondrial genome of Parasitidae (Parasitiformes: Mesostigmata). *International Journal of Acarology* 2022;**48**:645–53. https://doi.org/10.1080/01647954.2022.2164614

Ye F, Zhou J-Y, Li Z-Q. Evolutionary insights from the mitochondrial genomes of invasive scale insects (Hemiptera: Coccomorpha): large-scale transfer RNA gene truncations and tandem repeat-driven intraspecific gene rearrangements. *BMC Genomics* 2025;**26**:1003. https://doi.org/10.1186/s12864-025-12250-0

Yokobori S, Pääbo S. Transfer RNA editing in land snail mitochondria. *Proceedings of the National Academy of Sciences of*

Downloaded from academic.oup.com/zoolinnean/article/208/2/zlag163/9003135 by Università degli studi di Siena user on 28 October 2026

the United States of America 1995;**92**:10432–5. https://doi.org/10.1073/pnas.92.22.10432

Young SR, Block W. Experimental studies on the cold tolerance of *Alaskozetes antarcticus*. *Journal of Insect Physiology* 1980;**26**:189–200. https://doi.org/10.1016/0022-1910(80)90080-3

Yuan ML, Wei DD, Wang BJ *et al.* The complete mitochondrial genome of the citrus red mite *Panonychus citri* (Acari: Tetranychidae): high genome rearrangement and extremely truncated tRNAs. *BMC Genomics* 2010;**11**:597. https://doi.org/10.1186/1471-2164-11-597

Zhang DX, Hewitt GM. Insect mitochondrial control region: a review of its structure, evolution and usefulness in evolutionary studies. *Biochemical Systematics and Ecology* 1997;**25**:99–120. https://doi.org/10.1016/S0305-1978(96)00042-7

Downloaded from academic.oup.com/zoolinnean/article/208/2/zlag163/9003135 by Università degli studi di Siena user on 28 October 2026

© The Author(s) 2026. Published by Oxford University Press on behalf of The Linnean Society of London.
This is an Open Access article distributed under the terms of the Creative Commons Attribution License (https://creativecommons.org/licenses/by/4.0/), which permits unrestricted reuse, distribution, and reproduction in any medium, provided the original work is properly cited. Zoological Journal of the Linnean Society 2026 208(2) 1–20
https://doi.org/10.1093/zoolinnean/zlag163
Original Article